NAZARBAYEV UNIVERSITY

Bachelor of Engineering
(Mechanical Engineering)

DESIGNING AND BUILDING A HYBRID (ELECTRIC/IC) UAV

Final Capstone Project Report

By

Ruslan Baitlessov
Aitbek Myrzakhmet
Kuanysh Sharipov

Principal Supervisor: Desmond Adair
Co-Supervisor: Md Hazrat Ali

April, 2017

DECLARATION

We hereby declare that this report entitled "Designing and building a hybrid (electric/IC) UAV" is the result of our own project work except for quotations and citations which have been duly acknowledged. We also declare that it has not been previously or concurrently submitted for any other degree at Nazarbayev University.

Name: Aitbek Myrzakhmet

Date: 21.04.2017

Name: Kuanysh Sharipov

Date: 21.04.2017

Name: Ruslan Baitlessov

Date: 21.04.2017

ACKNOWLEDGEMENT

We would like to express our gratitude to our Capstone Project Supervisors: Professor Desmond Adair and Professor Md. Hazrat Ali for their trust in us, clear guidance and valuable feedbacks throughout the work on this project. We also want to thank Professor Luis Rojas-Solórzano for his help in assisting with performing simulations in Ansys software. Finally, we give our special thanks to the Capstone Project Coordinator, namely Professor Konstantinos Kostas for competent management of the overall process.

ABSTRACT

In comparison with conventional internal combustion (IC) engine power trains, a hybrid electric propulsion system with two or more energy sources has proved to be a more effective in terms of pollution rate, and a reduction of heat release and sound effects. For applications of hybrid electric/IC propulsion to vehicles and especially military, it has been demonstrated that considerable improvement of energy use by reducing fuel consumption required for basic functions occurs. Due to these factors, the use of unmanned aerial vehicles (UAVs) may be adopted to civil service as well. This might include detecting and monitoring disaster, hazards, and environment conditions, and reserving backup power for emergency. Based on the above information, this Capstone Project aims to develop the design a prototype of an economical and practical small scale tilt-rotor UAV, with emphasis on good performance characteristics, including high endurance, a rotor-tilting mechanism, payload capacity and vertical to horizontal transition stability. The main focus was on optimizing the aerodynamic parameters of fixed-wing prototype and combining the hovering abilities of a multi-rotor UAV. The CAD model built in SolidWorks, computational analysis and simulations of the vehicle performance in Ansys CFX related to this project are delivered as well. In addition, laboratory work was done in order to check performance of both the engine and generator.

TABLE OF CONTENTS

LIST OF TABLES

LIST OF FIGURES

LIST OF ABBREVIATIONS

AEW	Airborne Early Warning
AUM	All-up-mass
DOD	Department of Defense
DOF	Degree of Freedom
IC	Internal Combustion
UAV	Unmanned Aerial Vehicle
VTOL	Vertical Take-Off and Landing

NOMENCLATURE

Ω_i	Rotational speed of rotor
b_i	Thrust coefficient
k_i	Torque coefficient
U_{out}	Voltage output from generator
K	Angular speed constant
ω_m	Angular speed of motor
P_{out}	Power output
R_m	Resistance of motor
R	Rotation matrix from coordinate system S_b to S_f
$\mathbf{p}_f$	Position of UAV in $\boldsymbol{S_f}$
$\mathbf{v}_b$	Linear velocity vector presented in $\boldsymbol{S_b}$
$\bar{\boldsymbol{m}}$	Diagonal matrix $\mathbf{diag}(\boldsymbol{m})$
$\mathbf{g}_f$	Vector of acceleration of gravity in $\boldsymbol{S_f}$
$\boldsymbol{\omega}$	Angular velocity vector
$\boldsymbol{\Theta}$	Vector of Euler angles
I	Inertial matrix of UAV
$\boldsymbol{F}_{A,T}^{b}$	Vector of external force in coordinate $\boldsymbol{E_b}$
$\boldsymbol{F}_{A}^{b}$	Vector of external aerodynamic force in coordinate $\boldsymbol{E_b}$
$\boldsymbol{F}_{T}^{b}$	Vector of thrusts in coordinate $\boldsymbol{E_b}$
$\boldsymbol{\Gamma}_{A,T}$	external torque vector
$\boldsymbol{\Gamma}_{A}$	External aerodynamics torque vector
$\boldsymbol{\Gamma}_{T}$	External thrust torque vector
$\boldsymbol{J}(\boldsymbol{\Theta})$	Jacobian matrix
T_1	Thrust of the 1st motor
T_2	Thrust of the 2nd motor
T_3	Thrust of the 3rd motor
δ	Tilting angle of the1st and the 2nd motors

ξ	Tilting angle of the 3rd motor
Q_1	Torque of the1st motor
Q_2	Torque of the 2nd motor
Q_3	Torque of the 3rd motor
D_{t_b}	Drag of stabilizer
D_{w_b}	Drag of wing
L_{w_b}	Lift of wing
L_{t_b}	Lift of stabilizer
e	Efficiency
$\boldsymbol{T_{cruise}}$	Thrust during cruise
F_L	Lift force
C_L	Lift coefficient
A	Area of wing
ρ	Density of air
v	Velocity of UAV
c	Chord length of wing
L	Wingspan
$T_{cruisepermotor}$	Thrust per motor during cruise
C	Capacity of battery
$P_{total,cruise}$	Total cruise power usage
$e_{battery}$	Efficiency of battery capacity
e_{usage}	Efficiency of battery usage
V	Voltage of battery
Ah	Current usage in battery
x	State variables
a	Input variables
t	Time

CHAPTER1. INTRODUCTION

1.1. Background

According to the U.S. Department of Defense (DOD) an unmanned aerial vehicle (UAV) is defined as "A powered vehicle that does not carry a human operator, can be operated autonomously or remotely, can be expendable or recoverable, and can carry a lethal or nonlethal payload". General attributes of UAV are the following:

- Smaller size potential;
- High versatility;
- Greater performance than manned aircraft—design flexibility [5].

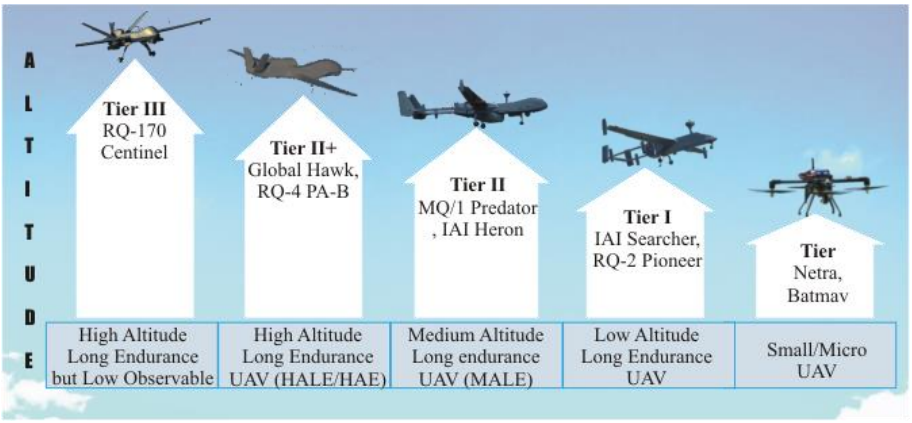

Figure 1.1. Different types of UAV according to classification [18]

Before looking into the characteristics of UAV in more detail, it is important to list common uses of these vehicles. The uses can be classified as follows:

Military uses

- Relaying radio signals;
- Protection of ports from offshore attack;
- Target designation and monitoring;
- Radar system jamming and destruction;
- Airfield damage assessment;

Civilian uses

- Aerial photography;
- Crop monitoring and spraying;
- Pollution and land monitoring;
- Fire detection, incident control [7]

There is a large number of features and characteristics that have been used to classify UAVs, including maximum take-off mass, operating conditions, capabilities, endurance or any combination of these and other characteristics. Table1.1 provides a comprehensive classification of UAV, where both a wide variety of UAV systems and capabilities as well as multiple ways of differentiation [9].

Table 1.1. Classification of UAV by altitude, range and endurance

Category	**Mass [kg]**	**Range [km]**	**Flight Altitude [m]**	**Endurance [h]**
Micro	<5	<10	250	1
Mini	<20/25/30/150	<10	150/250/300	<2
Close Range (CR)	25-150	10-30	3000	2-4
Short Range (SR)	50-250	30-70	3000	3-6
Medium Range (MR)	150-500	70-200	5000	6-10
MR Endurance (MRE)	500-1500	>500	8000	10-18
Low altitude deep penetration (LADP)	250–2500	>250	50–9000	0.5–1
Low altitude long endurance (LALE)	15–25	>500	3 000	>24
Medium altitude long endurance (MALE)	1000–1500	>500	3000	24–48

During the last two or three decades UAVs have experienced great development. Currently, two types of small UAV platforms dominate, namely fixed-wing conventional aircraft and rotary-wing Vertical Take-Off and Landing (VTOL) aircraft. There is a certain amount of inherent limitations associated with each type of UAV, such as flexibility, payload, endurance, and etc. However, the development of a fixed-wing VTOL UAV or so-called hybrid UAV, which can adopt both the ability of vertical take-off and landing as well as high cruising speed and enhanced endurance, and the ability to loiter, is a new promising trend that is taking place. Thus, the possibility of performing either wider range of missions or a better performance in the same missions becomes possible [24].

Due to the ability of such a hybrid UAV to act like either a fixed wing or rotary wing UAV, makes the use of such an aircraft very desirable in different missions despite its increased mechanical complexity and more difficult control features. Tilt-rotor UAVs are considered

as one of the most attractive and effective solutions because of their stability, energy efficiency and controllability [7].

1.2. Mission

A small UAV offers advantages, such as low cost for the airframe itself, low acoustic, visual and even the heat signatures for military purposes. Particularly, the latter one implies use of the UAV for land monitoring. The UAV will be advantageously used for aerial surveillance, with certain missions requiring no detection of the aircraft. It might include the following tasks, such as detecting and monitoring disaster, hazards, and environment conditions, and reserving backup power for emergency.

An aircraft mission usually consists of several flight phases with different requirements, such as take-off and climb, the cruise flight to and from the surveillance area, loitering (which may include descent and climb) and finally descent and landing. Generally, the mission profile for this UAV model is shown in the Figure below.

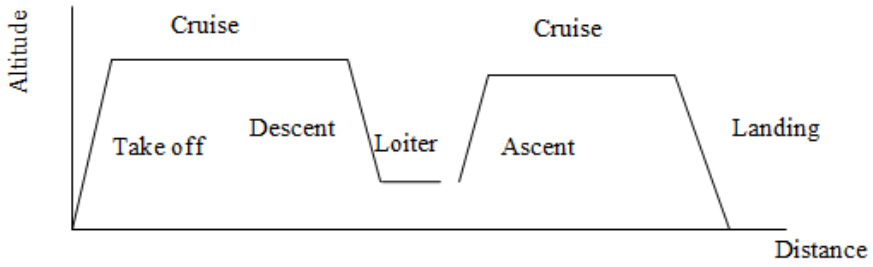

Figure 1.2. Mission profile

1.3. Objectives

Objectives of this project are based on requirements set by a mission of the UAV. An electric propulsion system itself would be the best choice for this objective, but such a choice strongly limits the endurance and range due to the low specific energy. Therefore, combination of electric with IC engine system is required [17].

An electric UAV has already been designed within the School of Engineering, Nazarbayev University, and the object of this further work is to investigate the feasibility of building on the skills and knowledge already researched and designing a similar UAV, which will have a much higher endurance capability, and a low acoustic/visual/heat signature. Despite the versatility of a helicopter in switching between several flights modes, its range and endurance is much less due to low energy conversion efficiency rotors and supersonic speed limitations at rotor tips for high cruise speeds. VTOL UAVs do not have these restrictions for forward flight, and also, providing the propeller radius is not large, the mechanical designs are usually simple [17].

In summary, the main objectives of this project are to design a prototype of an economical and practical small scale tilt-rotor UAV, with emphasis on good performance characteristics that are listed below. These include:

- Endurance
- Rotor tilting mechanism
- Payload capacity
- Vertical to horizontal transition stability
- Ease of repair and maintenance

Since the project aims to provide a design of a UAV with good performance, the main focus will be on improving performance by optimizing the aerodynamic parameters of the fixed-wing prototype and combining the hovering abilities of a multi-rotor UAV. Based on findings of the preliminary literature review and discussion with the experts, the realistic and challenging design requirements were defined (Table 1.2). Particularly, the 2nd chapter will contain information on these findings.

Table 1.2. Design requirements

Payload	Up to 900 g. This value includes the mass of the camera and a lightweight gimbal.
Endurance	1.5 hours. The endurance has to be somewhere between 1 and 2 hours, being comparable with typical fixed-wing UAVs with hybrid propulsion system
Wingspan	2-2.5 m. The span of the UAV should be appropriate for convenient transportation and allow its exploration in urban areas.
Mass	Up to 10 kg
Operating altitude	100-300 m
Durability and reliability	To be able to operate in severe weather conditions and to withstand wind gusts.
Flight regime	To be able to operate in both RC and autonomous waypoint navigation regimes.

CHAPTER2. LITERATURE REVIEW

2.1. Design stages

According to [4], the design of a UAV will usually consist of three stages:

1) *Development of concept*

Conceptualization is a phase of brainstorming ideas and analysis of advantages and disadvantages of implementing those ideas. In this part, potential solutions must be presented for existing problems. Morphological analysis technique includes specific design parameters listed in a table and various solutions for each problem. Finally, different alternatives will be evaluated between each other to identify possible strengths and weakness [27].

2) *Preliminary design*

Preliminary design includes different alternatives for overall system configuration, which includes sketches, schematics, diagrams and layouts of the project. During this phase parameters of created parts are concentrated on the overall framework of the model. However, it is not sufficient for the final model [20].

3) *Detailed design*

Detailed design stage includes each aspect of the product and its complete description, which include CAD models, simulations, drawings, final characteristics and calculations [10].

There are other phases after the detailed design stage which include manufacturability factors and modifications followed by continued improvements of the UAV. This report is concentrated on the preliminary three stages mentioned above.

2.2. Fixed-wing aircraft

During a flight, a fixed-wing aircraft is subjected to basic forces like thrust, drag, weight and lift. The primary goal of fixed-wing aircraft is to create enough lift for takeoff and

landing as well as to provide sufficient lift to remain at a constant altitude during the cruise. The reaction force (the vertical component of the lift force) is in the opposite direction and opposes the gravitational force.

The Figure2.1 represents an aircraft travelling with some velocity in a horizontal direction. A difference of aerodynamic pressures between the upper (suction) and lower (pressure) surfaces of the aircraft's wings is a key to providing lift. Specifically, the lower pressure on the upper surface and the higher pressure on the lower surface of a wing create the reaction force (lift). In order to create sufficient lift there must be enough thrust to overcome a drag. This drag consists of two components, namely skin friction and pressure difference between rear and front sides of the wing. Its impact with a small horizontal component of thrust resists the motion of the aircraft. Thus, minimization of the drag has a crucial role for fixed-wing UAV to increase its efficiency [12].

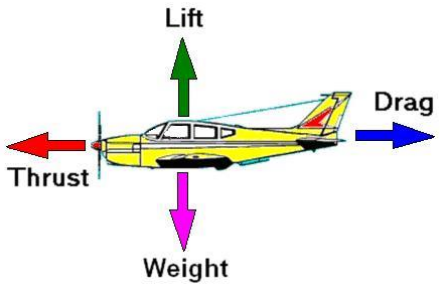

Figure 2.1. Forces acting on a plane [26]

2.3. Rotary-wing Aerodynamics

The rotary-wing aircraft aerodynamics is more complex than that of the fixed-wing one. The method of achieving lift force on rotary wings is basically the same as for the fixed-wing. The main difference is ability for the vertical take-off and landing of the rotary-wing aircraft.

In a rotary-wing system lift is produced by angle of incidence and angle of attack (figure 2.2). Angle of incidence located between chord line of a blade and the rotor hub. Angle of attack (AOA) located between airfoil chord line and resultant relative wind. Figure2.2 illustrates velocity distribution of along the blades.

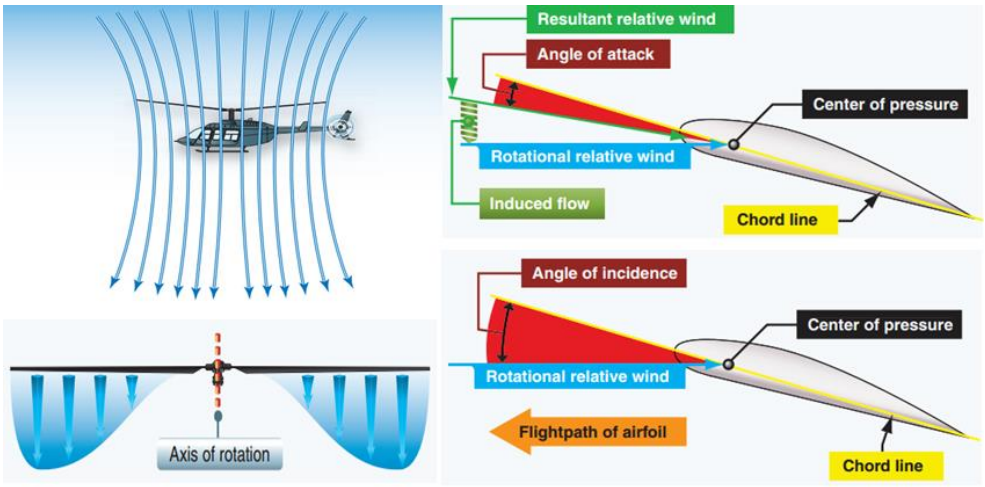

Figure 2.2. Normal induced flow velocities along the blade span during hovering flight: a) Induced flow, c) velocity distribution along the blade. Rotor blade angles: b) AOA d) angle of Incidence [13]

2.4. Payload

Besides the size and mass, the maximum payload and its extra requirement for energy define the primary layout, size and all-up-mass (AUM) of the UAV. The payload is important as it is connected with main reasons for construction and designing of the UAV. Depending on the purpose payloads can be varied from a kilogram up to thousand kilograms and from a few cubic centimeters to more than a cubic meter in volume. Also, position of the payload is important, since it has significant influence on the configuration and model of the UAV frame. In our case, placement of an imaging camera should be in such a way that it would have the best view of the landscape. Payloads must be placed around the center of mass of the UAV.

2.5. Endurance

The endurance of the UAV, depending on the requirements, can vary from 1 hour to more than 24 hours for a long-range surveillance or airborne early warning (AEW) system. Hence, the volume and mass of the fuel or battery load are strongly related to the endurance and efficiency of the aircraft aerodynamics. Thus, the mass of fuel can range between 10% and 50% of UAV's AUM, depending on its mission, which has a directly connected

influence on the endurance. Therefore, amount of fuel should be taken into consideration during design in order to fit the required endurance.

2.6. Development of concept

In order to create a reference point for the initial calculations, the characteristics of UAV have to be set. This was done by studying different existing small-scale UAVs designed for civilian missions. According to [24], there is only one prototype of UAV with a hybrid IC engine and electric propulsion system built at the US Air Force Institute of Technology. Despite the fact that several university projects treated the design/construction of hybrid-electric propulsion systems there appears to be no information about design requirements or characteristics of their UAVs. Table2.1 below gives design requirements for UAV mentioned above.

Table 2.1. Mission and aircraft design requirements for UAV built in US Air Force Institute of Technology

Parameter	Value	Units
Endurance (t_{endur})	3	hr
One way cruise time (t_{cruise})	1	hr
Cruise velocity (V_{cruise})	20.5	m/s
Max velocity (V_{max})	30.9	m/s
Rate of climb (ROC)	2.03	m/s
Take-off altitude MSL (h_{TO})	1500	m
Mission altitude AGL (h)	300	m
Max gross takeoff mass (m_{TO})	13.6	kg
Payload mass (m_{pay})	2.27	kg
Payload power (P_{pay})	25	W
Flight control system power (P_{FCS})	10	W
Zero-lift drag coefficient ($C_{D.O}$)	0.036	
Oswald span efficiency factor (e)	0.85	

In order to identify a reference UAV with certain characteristics, the examples of current small UAVs have to be analyzed. Table2.2 illustrates some existing models with either an electric motor or IC engine propulsion system [19]. As can be seen from this table, smaller

UAVs generally have an electric propulsion system with limited flight time, while IC-powered UAVs have longer endurance, but higher take-off mass.

Table 2.2. The characteristics of reference UAVs

Model name	Company	Power plant	Weight, lbs	Span, inches	Endurance, min
Raven B	AeroVironment, Inc.	Electric motor	4.2	53	90
Puma	AeroVironment, Inc.	Electric motor	13	102	150
Stalker	Lockheed Martin	Electric motor	14	120	120
Desert Hawk IIII	Lockheed Martin	Electric motor	6.5	54	90
Silver Fox	Advanced Ceramics Research	Gas engine	26.2	94	600
Scan Eagle	Boeing	Gas engine	39.6	120	900

As it can be seen from the Table 2.2, a wing span ranges between 53 and 120 inches or 1.35-3 m, whereas a weight of 4.2-39.6 lbs or 1.89-17.8 kg gives a reference point for initial sizing and weight calculations. Regarding the endurance, its value for a hybrid UAV can fluctuate between 90 and 900 min.

CHAPTER3. PRELIMINARY DESIGN

3.1. Alternative 1

An initial concept of the small-scale UAV was chosen to be a multi-copter (Figures3.1-3.2.), particularly quad-rotor. The main reasons for using this arrangement rather than a tri-copter are:

- simplicity (a quad-rotor looks like a simple cross with four identical motors),
- control system (quad-rotors are symmetrical, therefore a simpler control setup is required), and
- reliability (due to their mechanical simplicity, quadrotors could withstand a crash much better than tri-copters).

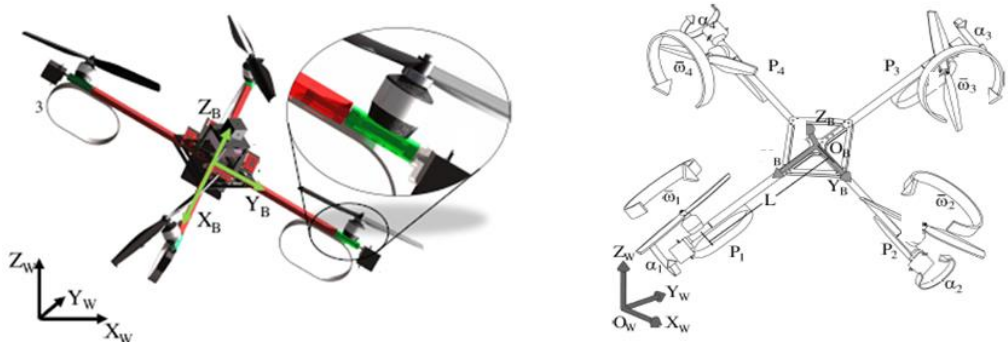

Figure 3.1. Quad-rotor UAV concept [23]

Figure 3.2. Schematic view of the propellers quad-rotor concept model [23]

However, there are several limitations associated with quad-rotor UAVs in comparison with VTOL UAVs. The former involve greater mechanical and electronic complexity, which in turn leads to more complicated maintenance and repair processes. Thereby, the user's operational endurance will be decreased, which can cause an increase in operational costs. Due to lower speeds and shorter flight ranges for multi-copter UAVs, some additional flights for surveying certain significant areas are required, and thus increase in time and operational costs take place [23].

3.2. Alternative 2

The first alternative is inefficient and not suitable for long-distance deployment for our purposes and characteristics. It was therefore decided to investigate the alternative shown in Figure3.3. This consists of a fuselage, 3 propellers, 3 motors, clutch, controllers, etc. Due to limits on the mass of the prototype, flight time and maximum altitude, and to provide stability, and, rolling, yawing and pitching capability, the number of motors was chosen to be 3. In order to decrease the noise generated due to motors, 2 motors located ahead of the wings can be switched from IC engine at the take-off to battery powered during cruise and loitering. During cruise these two motors plus related propellers have to tilt by 90 degrees so that a horizontal driving thrust is applied.

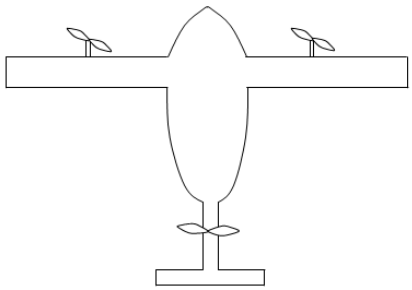

Figure 3.3. Alternative 2 Design

According to the objectives of the UAV's concept, it should be VTOL. During takeoff all three motors are vectored as illustrated in the Figure3.3 in order to have enough vertical thrust to overcome the aircraft's weight and prove a small vertical acceleration; in addition to providing stability. This second alternative has however several disadvantages with efficiency and for our UAV this is highly significant, as this influences the endurance. Considering this design, the propeller rotates above the wing of the aircraft and around 40% of its area is above the wing. Also, the width of wing is approximately 10 inch according the size of our UAV. Analyzing the aerodynamics, it can be clear that a propeller above the wing has less effective thrust since it creates an additional vertical drag on the surface of the wing by the air flow downwards. This is the case for the two front propellers. Therefore, this design is considered as less effective [4].

In order to solve these problems our group proposed a solution. The motors will turn 90 degrees with the wing. This would significantly decrease thrust losses and cancels blockage of the air flow by the wing. It was a good solution for small diameter propellers. The proposed diameter of one propeller is however 20 inches in diameter and the length of the wing is around 80 inches. This means that the wing has two sections with 20 inch lengths to be turned with the motors. This causes doubts on the rigidity of our system which can be simply destroyed. Thus, the second alternative with turning wings during vertical takeoff is considered unreliable.

3.3. Alternative 3

The third alternative, considered to be the best option for the vertical takeoff and for cruise, is a variation of the aircraft shown in Figure3.4. This figure represents the shape of the airframe. This concept will be taken to construct our UAV. The only similarity with the second alternative is that the third motor will be located between the tails of the rear part. There is inefficiency with the geometry resulting in additional drag, namely form drag and a small increase in skin friction drag.

Figure 3.4. Alternative 3 Design [5]

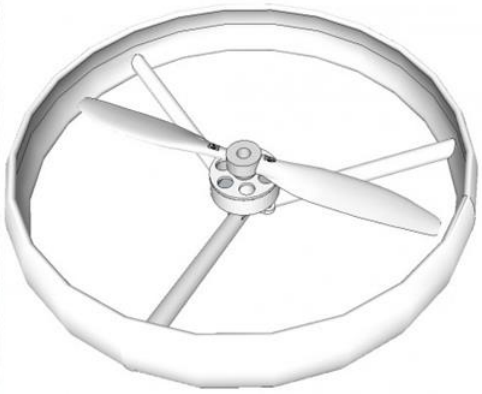

Figure 3.5. Propeller guard [22]

Figure 3.5 presents a propeller guard. It provides a fixed ring around the propeller and fixed by the frame. It saves the propeller from direct contact of the UAV. Such guards are often used and made from plastic. In our case, it has been decided not to use guards. There are several reasons for such a decision:

1) High source of vibration (the risk of propeller and guard collapse)
2) works only for low force impacts
3) Decrease thrust in case of many supports under the propeller

3.4. Hybrid Propulsion system

Propulsion system of a hybrid UAV can be classified into five categories. They are series hybrid, parallel hybrid, series-parallel hybrid, complex hybrid, and fuel cell hybrid [18].

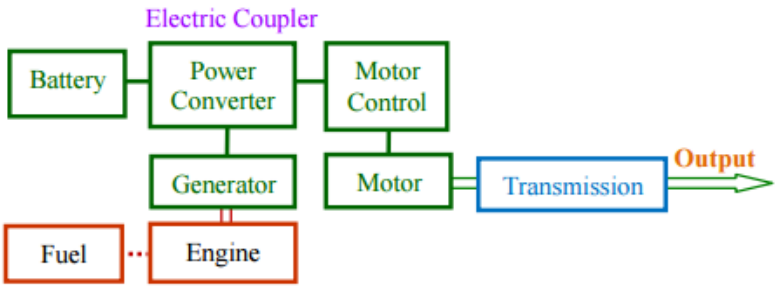

Figure 3.6. Series propulsion system

In Series propulsion (Figure3.6) our engine is connected to the generator, which supplies electric motor with electricity. Also, the motor can be supplied via battery. This system can be powered by battery and engine (IC) individually and simultaneously. The engine is a primary source of energy.

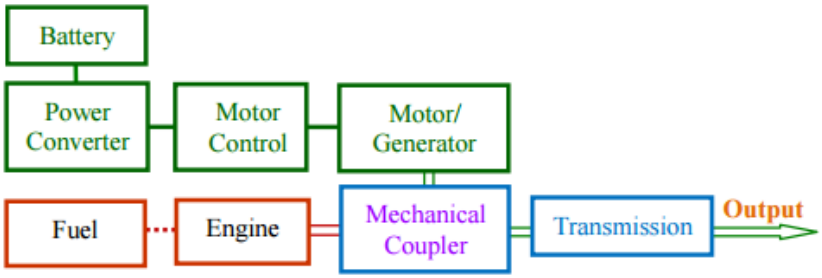

Figure 3.7. Parallel propulsion system

Figure3.7 represents a parallel propulsion system, where the mechanical coupling system realizes transmission of power. It can work individually and simultaneously by battery and engine. The primary source of energy is the engine.

According to our design the UAV has three propellers. Therefore, parallel propulsion system usage will be ineffective, as additional coupling systems would be added, which

adds additional weight. It would be effective in the case of one propeller usage. However, in our case series propulsion has an advantage over a parallel one. The engine will be used to produce electricity and it will supply all three motors with electricity through cables, which are lightweight [18].

3.5. Role of tail rotor

An aircraft inflight is free to rotate in three dimensions. This increases the complexity of structure and stabilizing. The rotations are done about the principle axes, as shown in Figure3.8, and are pitching, nose up or down about the wing to the wing axis; rolling, rotation about axis from nose to tail; yawing, rotating nose right or left about axis perpendicular to both roll and pitch axes.

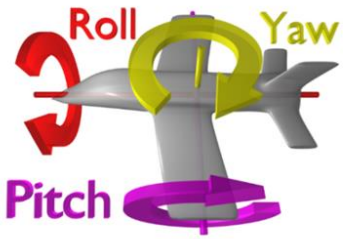

Figure 3.8. Pitch, roll and yaw in an aircraft [29]

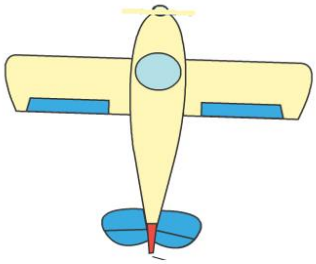

Figure 3.9. Control surfaces: red, for yaw; blue, on the tail and on the wings, are for pitching and rolling respectively [29]

In order to keep an aircraft stable, adjustment of roll, pitch and yaw angles has to be made. These can be done by producing toque about the principle axes. The torque can be produced by flexible control surfaces on the aircraft as shown in the Figure3.9.

Adding these control surfaces increases the number of moving components and decreases the rigidity of the frame. Thus, an alternative for rotating the plane was considered to be the tail rotor. The tail rotor will have two degrees of freedom: one to cause yawing and another to cause pitching. For instance, in order to make aircraft turn (yaw) to the left the tail rotor should be tilted as shown in Figure 3.10.

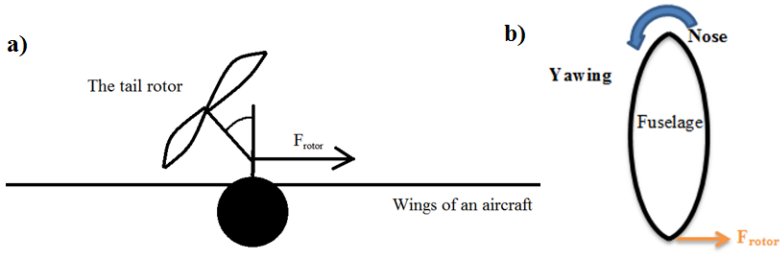

Figure 3.10. View of the aircraft with rotor tilt: a) Rear view, b) Top view

Tilting the tail rotor creates force F_{rotor} exerted at the tail causing the aircraft to yaw. However, a rolling also occurs due to pressure difference on wings caused by yaw. The lift forces on the wings change as in the Figure 3.11.

$$L_{starboard} > L_{port}$$

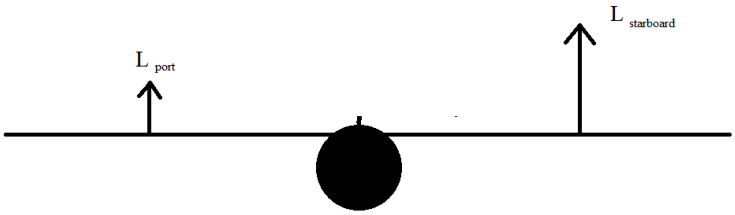

Figure 3.11. Rear side view of the aircraft with lift forces on wings

Therefore, starboard arises and aircraft rolls as well as yaws.

3.6. Mass estimation

The total mass of the UAV can be calculated by summing masses of all components. It should be noticed that the payload has to be included as well, and therefore the total take-off mass is to be calculated. The Table3.1 below contains description of each component, its mass, quantity and the total mass as well.

Table 3.1. Mass estimation of the model

Item #	Description	Mass per unit, kg	Amount	Mass, kg
Motor	T Motor U8 Pro KV 170	0.240	3	0.72
Motor	T Motor U11 KV 120	0.730	1	0.73
Gas engine	55cc Gas Engine	1.31	1	1.31
Gas propeller	Turnigy 3D Gas Propeller 20x6	0.115	3	0.34
Flight Controller	ArduPilot Mega APM2.6 Flight Controller	0.040	1	0.04

Servo motor	Turnigy™ TGY-306G-HV Ultra Fast	0.021	5	0.11
Electric speed controller	ESC 6-12s 40A	0.055	3	0.17
Electric speed controller	ESC 6-12s 60A	0.060	1	0.06
Battery	Multistar 12s 4000mAh	0.620	2	1.24
FrySky Telemetry	FrySky 24GHz Combo Digital Temetary Radio System Mode 2	0.070	1	0.06
Resin	Epoxy resin APH 161	0.025	1	0.03
frame	plastic	1.620	1	1.92
payload	camera	0.800	1	0.80
Total mass				**7.53**

3.7. Thrust/torque coefficients

According to [30], the forces T_i and reactive torques Q_i can be approximated by

$$T_i = b_i \Omega_i^2 \qquad 3.1$$

$$Q_i = k_i \Omega_i^2 \qquad 3.2$$

These factors are thrust and torque coefficients respectively. In order to find these coefficients, values for both thrust and torque depending on rotational speed of the motor have to be listed (Tables 3.2-3.3). These parameters can be found from [4], where thrust values are given for the U8 pro KV170 motor (used in this project).With regard to torque, there is no information on its values for the same motor, however, similar values for U10 motor are found. Both plotted graphs (dependence of coefficients on motor's rotational speed) and average values for coefficients are obtained below using previous information and Microsoft Excel software.

Table 3.2. U8 pro KV170 motor specifications

Frequency, rpm	Thrust, g	Thrust, N	Angular speed, rad/s	Coefficient, N/(rad/s)^2
3350	2250	22,07	350,63	1,80E-04
4100	3640	35,71	429,13	1,94E-04
4500	4630	45,42	471,00	2,05E-04
4900	5500	53,96	512,87	2,05E-04
5550	6780	66,51	580,90	1,97E-04
			average	**1,96E-04**

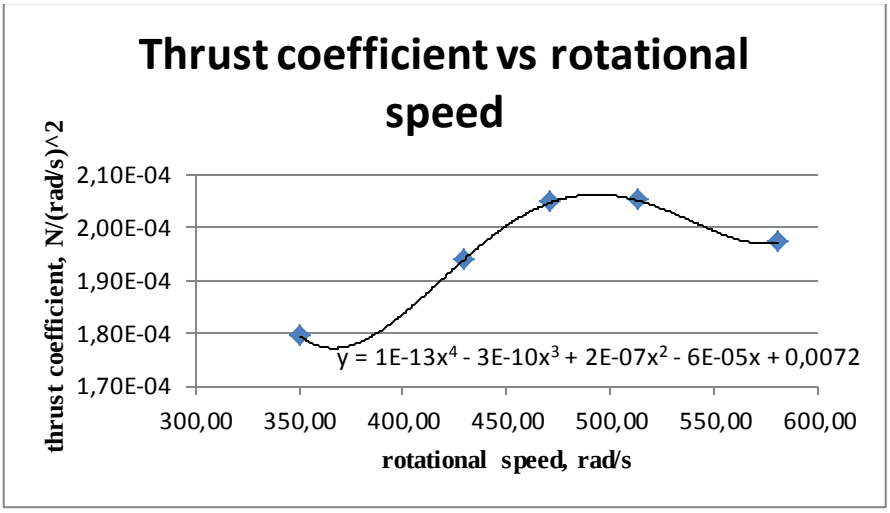

Figure 3.12. Thrust coefficient vs speed

Table 3.3. U10 KV80 motor specifications

Frequency, rpm	Torque, N*m	angular speed, rad/s	Coefficient, N*m/(rad/s)^2
2163	0,69	2,26E+02	1,34E-05
2363	0,81	2,47E+02	1,33E-05
2545	0,94	2,66E+02	1,32E-05
2746	1,10	2,87E+02	1,33E-05
3078	1,38	3,22E+02	1,33E-05
3342	1,71	3,50E+02	1,40E-05
3906	2,27	4,09E+02	1,36E-05
		average	1,34E-05

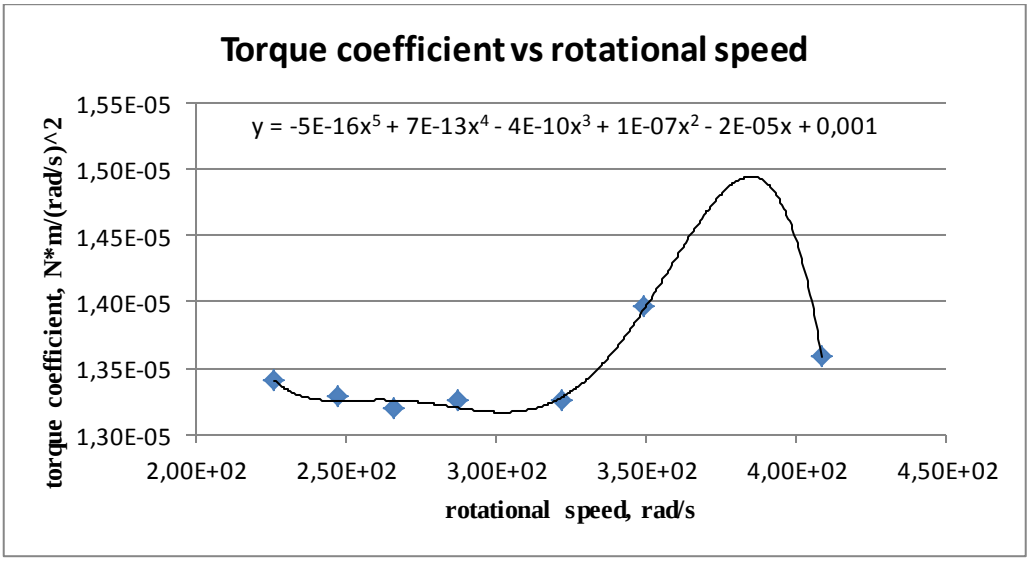

Figure 3.13. Torque coefficient vs rotational speed

CHAPTER4. LABORATORY WORK

The practical part of this project was planned to include building and testing the full model of the aircraft. However, due to the budget limitation it is not possible. The decision was made to conduct an experimental work within our budget. The aim of the experiment is to test the IC and generator in terms of efficiency and compatibility. Also, the ability of the generator to work as a starter can be tested. There were not found any reliable sources of information about the Permanent Magnet Brushless Outrunner generators. This experiment will clarify the performance of the generator and support or refute our assumptions used in calculations.

4.1. Theoretical background

Permanent magnet brushless motors can work in reverse, as generators. The power input rotates the rotor of the generator, on which the permanent magnets are placed. On the stator, there are a number of windings which produce EMF when there is a magnetic flux change passing through them according to the Faraday's law (the Figure4.1.). The motor is designed to give a certain amount of rotational speed per voltage applied, so called KV. Thus, the voltage output of the generator is linearly proportional to the rotational speed of the rotor. Furthermore, the output of the generator is three phase voltage. In order to convert this into DC the 3-phase rectifier is needed.

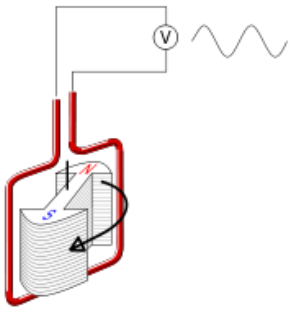

Figure 4.1. Diagram of a simple alternator

The start of the RC IC engine is done in two ways: manual and by auxiliary unit. In our case, we need the engine to be started by the motor/generator. The challenge is to check whether the motor can start the engine and to be able to stop the motor by the moment the IC engine can keep itself running. Otherwise, the voltage generated by IC engine may pass through ESC controller in reverse direction and cause damage.

The voltage generated is directly proportional to the speed of the motor. The DC motor we have has a rating of 170 KV which means when given 1 V it will rotate with 170 RPM. This is assumed to work both ways.

$$U_{out} = K * \omega_m \qquad 4.1$$

where K is 170.

Resistors have 120 k Ω and 1000 k Ω. The different loads were applied in order to observe any dependency on the load. To calculate the power output simple equation can be used:

$$P_{out} = \frac{{U_{out}}^2}{R_m} \qquad 4.2$$

4.2. Experimental setup

The results of this experiment will have an effect on the project. The main calculations of this project are based on the assumptions about the results of this experiment. However, due to the budget limitation we cannot conduct the experiment with the parts that we decided to use in the final model. Thus, the cheaper units with lower power rating will be used as test subjects. It is assumed that with the same manufacturer of the parts the test results would be similar. Though, this assumption must be made with caution, since the performance of the generator and engine might vary with the size or power rating factor.

Equipment needs the following parts listed in the Table 4.1 below.

Table 4.1. List of parts needed for the experiment

#	name	#	name	#	name
1	2-stroke IC engine	7	Power source	13	Servomotor
2	Flexible coupling	8	Cooling fan	14	Gasoline tank
3	DC motor	9	Kill switch	15	Gasoline
4	Rectifier	10	Battery	16	Arduino/Processing software
5	Multimeter	11	Rigid frame	17	Engine oil
6	ESC for DC motor	12	Tachometer	18	Resistors

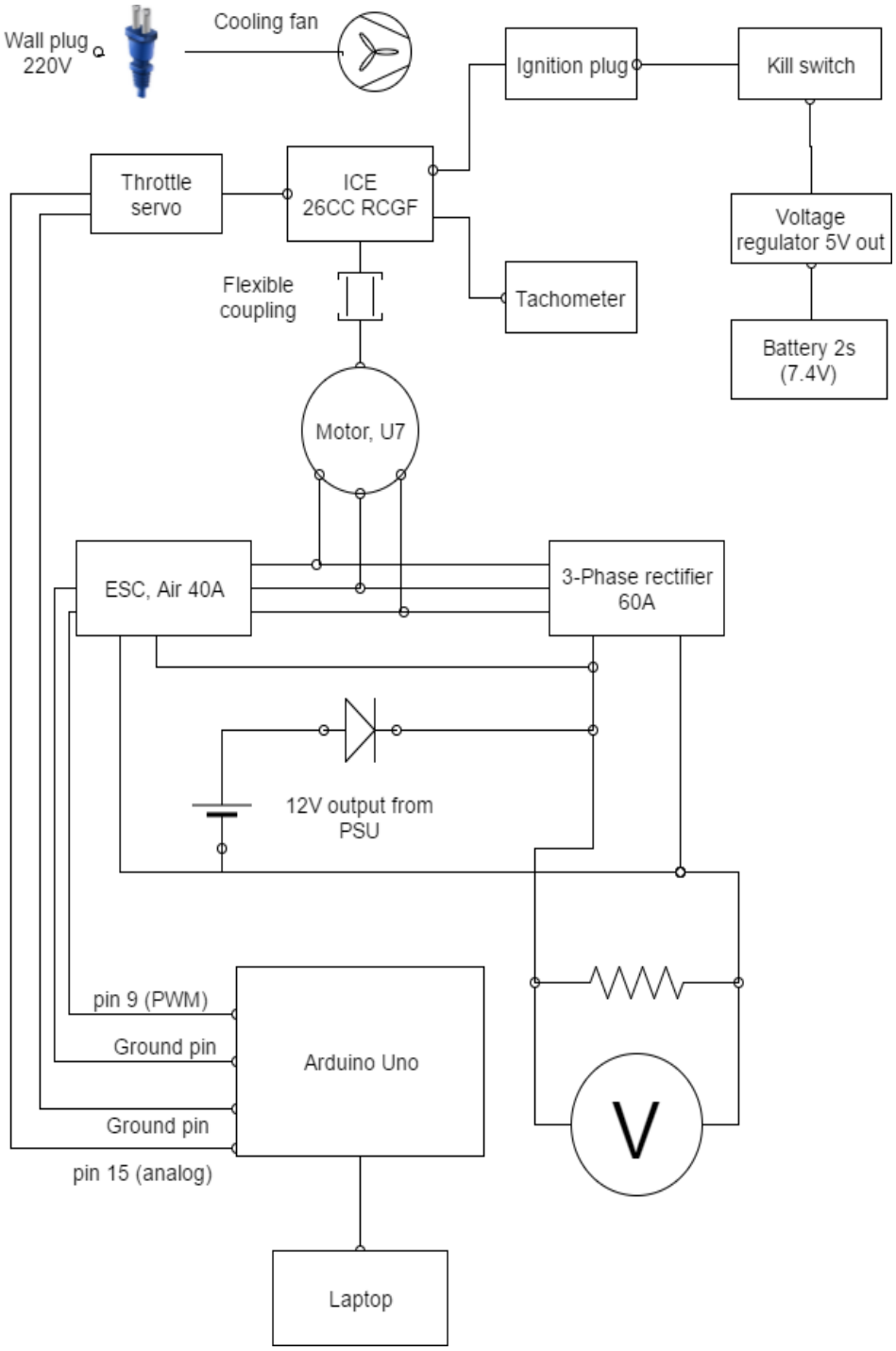

Figure 4.2. Detailed schematic of the laboratory setup

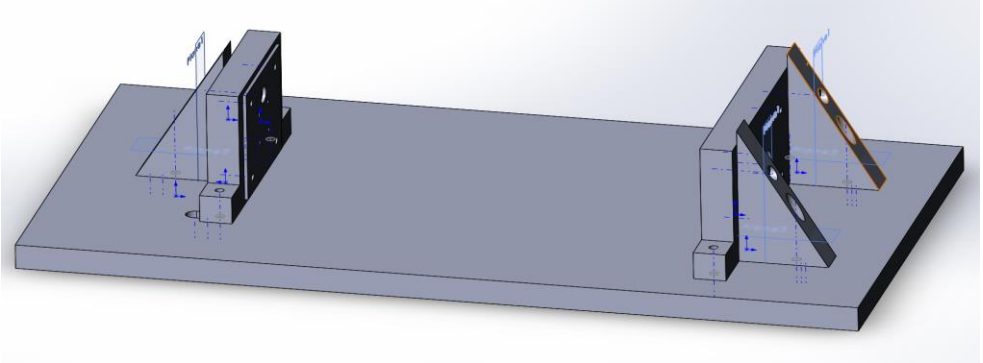

Figure 4.3. Stand for motor and engine connection

The stand from the Figure4.3 was made of wood. This was designed assuming that the motor will be able to start the engine. This rig is then placed on rigid base connecting via rubber to allow vibration energy to dissipate.

4.3. Procedure

First, start with mounting everything on its place and connect necessary wirings, according to Figure4.2, except for power sources (batteries, wall plugs). Then, prepare fuel for IC engine and fill the gasoline tank. The preparation of the fuel is done by mixing the gasoline with engine oil (2-stroke) in proportion of 30:1 accordingly. This process should be done with care as it includes flammable liquids. After that, connect the fuel line to the engine and connect all the power units to the circuit. Double check the Kill switch, because it is the measure to stop the engine on demand.

An Arduino board was used to control throttle servo and DC motor remotely from the computer. In order to do this Arduino software is necessary and to control the output with mouse "Processing" open source software was installed. The Arduino board can be connected via USB cable providing power and input signals. If throttle servo and DC motor is connected as in the scheme provided the codes in the appendix can be executed on Arduino and Processing software. The code will transfer mouse movement in "x" and "y" directions into servo and motor movement. Also there is an option that will give motor high signal when the mouse button is pressed. This helps with starting the engine as it requires high acceleration for a small fraction of time.

To begin the experiment start the engine pressing the mouse for short amount of time until the engine runs itself. Then fill the Table1 in appendix by varying throttle and changing resistance. The readings are taken from tachometer and voltmeter. When finished, stop the engine using kill switch.

4.4. Results

The motor could not overcome the resistance of the piston friction and air compression. The engine lacked starting power and was unable to start. This was due to the low voltage supply to the motor. The power source for the motor was 12V whereas the motor is suggested to work with 22.2 V source. The reason for using 12V instead of 22.2V was that recommended battery was not available.

However, we were able to control servo motor and DC motor through laptop. Also before the test the DC motor was manually turned which generated small amount of voltage that was seen on the voltmeter. Before installing everything on the stand, the IC engine was tested to ensure it can be started and held running. The result was that given engine worked as expected.

4.5. Conclusion

The preliminary tests of the engine and electrical scheme indicated that both are capable of producing results. The power supply to the DC motor of 12V did not produce enough torque to start the engine. The unavailability of the battery was mainly due to prohibit of battery transport with standard customer shipping method.

CHAPTER5. CONTROL SYSTEM

5.1. Mathematical modeling

The following assumptions are made to obtain the equations of motion:

- The UAV was assumed to be rigid.
- This section gives the development of the 6-degrees-of-freedom non-linear equations.
- The UAV is free to rotate and translate in 3D space.
- There are no ailerons, elevator or rudder.
- Pitch, yaw and roll during horizontal fight effected using rotor 3 (rear).
- During vertical Take-off & Landing or hovering speed of aircraft assumed small no aerodynamic forces or torques present.
- This analysis is carried out using the geodetic coordinate system.
- No wind was assumed during the development of equations

The following equations are found using attached diagram below (Figure 5.1). Center of gravity is placed at the vortex of T-frame, while the distance between the centers of lift and gravity is equal to ¼ of the chord length.

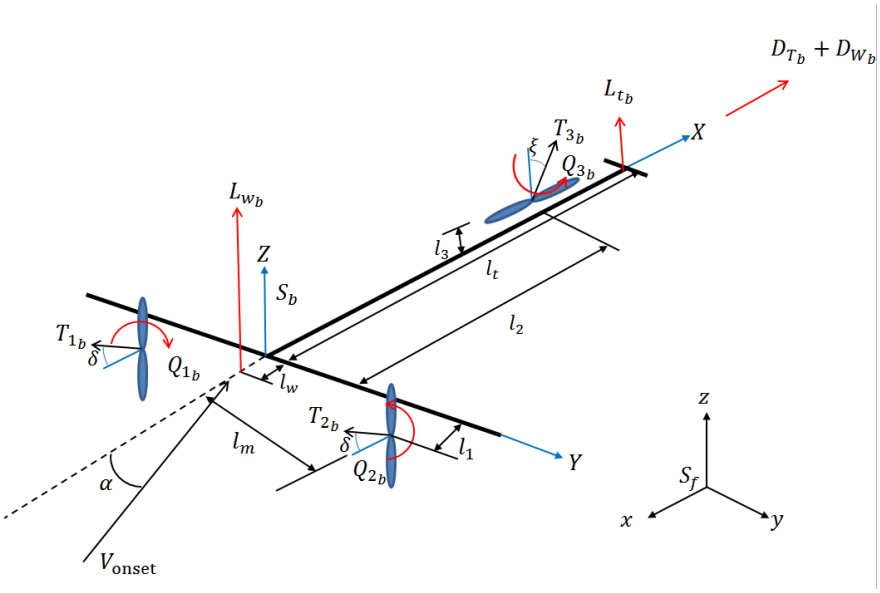

Figure 5.1. Configuration of the UAV model with reference and body frames

According to [30], the Newton-Euler equations of motion describing the six degrees of freedom of the system can be separated into translational motion ($\sum P$) and rotational motion ($\sum M$):

$$\sum P: \begin{cases} \dot{\boldsymbol{p}}_f = \boldsymbol{R}\boldsymbol{v}_b \\ \boldsymbol{v}_b = \boldsymbol{R}^T \boldsymbol{g}_f + \frac{1}{m}\boldsymbol{F}_{A,T}^b - \boldsymbol{\omega} \times \boldsymbol{v}_b \end{cases} \qquad 5.1$$

$$\sum M: \begin{cases} \dot{\Theta} = J(\Theta)\boldsymbol{\omega} \\ I\dot{\boldsymbol{\omega}} = -\boldsymbol{\omega} \times I\boldsymbol{\omega} + \boldsymbol{\Gamma}_{A,T} \end{cases} \qquad 5.2$$

$$J(\Theta) = \begin{pmatrix} 1 & tan\,\theta\, sin\,\phi & tan\,\theta\, cos\,\phi \\ 0 & cos\,\phi & -sin\,\phi \\ 0 & \frac{sin\,\phi}{cos\,\theta} & \frac{cos\,\phi}{cos\,\theta} \end{pmatrix} \qquad 5.3$$

$$\boldsymbol{F}_{A,T}^b = \boldsymbol{F}_A^b + \boldsymbol{F}_T^b \qquad 5.4$$

To avoid singularity ($-\pi/4 \leq \theta \leq \pi/4$) and the Euler angles are used to represent the attitude due to their simplicity.

Each motor produces a force T_i parallel to its axis of rotation and a reactive torque Q_i opposite to the direction of rotation. The combination of the forces T_i and the reactive torques Q_i is given by

$$\boldsymbol{F}_T^b = [(T_1 + T_2)\,cos\,\delta \quad T_3\,sin\,\xi \quad (T_1 + T_2)\,sin\,\delta + T_3\,cos\,\xi]^T \qquad 5.5$$

$$\boldsymbol{\Gamma}_T = \begin{bmatrix} (T_2 - T_1)l_m\,sin\,\delta + (Q_2 - Q_1)\,cos\,\delta + T_3 l_3\,sin\,\xi \\ T_3 l_2 cos\,\xi - (T_1 + T_2)l_1\,sin\,\delta + Q_3\,sin\,\xi \\ (T_1 - T_2)l_m\,cos\,\delta + (Q_2 - Q_1)\,sin\,\delta + T_3 l_2\,sin\,\xi + Q_3\,cos\,\xi \end{bmatrix} \qquad 5.6$$

The aerodynamic forces $\boldsymbol{F}_{A,T}^b$ and torques $\boldsymbol{\Gamma}_A$ depend on the working mode of the aircraft.

In transition and horizontal phases the air velocity will be equal to the relative velocity of the UAV but in the opposite direction so

$$\boldsymbol{V}_{onset} = -\boldsymbol{V} \qquad 5.7$$

The vector of the onset velocity creates with the UAV an angle of attack (AOA) of α

$$\boldsymbol{F}_A^b = \begin{bmatrix} -D_{t_b} - D_{w_b} \\ 0 \\ L_{w_b} + L_{t_b} \end{bmatrix} \qquad 5.8$$

$$\boldsymbol{\Gamma}_A = [0 \quad L_{t_b} l_t - L_{w_b} l_w \quad 0]^T \qquad 5.9$$

The following 2 modes will be considered: vertical (tilt angle δ=90°), and horizontal (δ=0°, $T_3 = Q_3 = 0$).

For the vertical mode, only thrust forces have effect on motion; therefore $\boldsymbol{F}_{A,T}^b = \boldsymbol{F}_T^b \; and \; \boldsymbol{\Gamma}_{A,T} = \boldsymbol{\Gamma}_T$

$$\boldsymbol{F}_{A,T}^b = \boldsymbol{F}_T^b = \begin{bmatrix} 0 \\ T_3 \, sin\, \xi \\ (T_1 + T_2) + T_3 \, cos\, \xi \end{bmatrix} \qquad 5.10$$

$$\boldsymbol{\Gamma}_{A,T} = \boldsymbol{\Gamma}_T = \begin{bmatrix} (T_2 - T_1) l_m + T_3 l_3 \, sin\, \xi \\ T_3 l_2 \, cos\, \xi - (T_1 + T_2) l_1 + Q_3 \, sin\, \xi \\ (Q_2 - Q_1) + T_3 l_2 \, sin\, \xi + Q_3 \, cos\, \xi \end{bmatrix} \qquad 5.11$$

For the horizontal mode, both thrust and aerodynamic forces contribute to the motion

$$\boldsymbol{F}_T^b = \begin{bmatrix} T_1 + T_2 \\ 0 \\ 0 \end{bmatrix} \qquad 5.12$$

$$\boldsymbol{\Gamma}_T = \begin{bmatrix} Q_2 - Q_1 \\ 0 \\ (T_1 - T_2) l_m \end{bmatrix} \qquad 5.13$$

$$\boldsymbol{F}_{A,T}^{b} = \begin{bmatrix} T_1 + T_2 - D_{t_b} - D_{w_b} \\ 0 \\ L_{w_b} + L_{t_b} \end{bmatrix} \qquad 5.14$$

$$\boldsymbol{\Gamma}_{A,T} = \begin{bmatrix} Q_2 - Q_1 \\ L_{t_b} l_t - L_{w_b} l_w \\ (T_1 - T_2) l_m \end{bmatrix} \qquad 5.15$$

A dynamic relationship is formed in order to obtain the nonlinear dynamics of the motion:

$$\dot{x} = F(x, a, t) \qquad 5.16$$

Table 5.1. State variables for motion model, x=[u v w p q r ϕ Θ ψ x_e y_e z_e] T

DYNAMICS						KINEMATICS					
TRANSLATION (m/s)			ROTATION (rad/s)			ROTATION (rad)			TRANSLATION (m)		
u	v	w	p	q	R	ϕ	Θ	ψ	x_e	y_e	z_e

Table 5.2. Input variables for motion model, a=[$\boldsymbol{F}_{A,T}^{b}$ $\boldsymbol{\Gamma}_{A,T}$]

FORCES	MOMENTS
$\boldsymbol{F}_{A,T}^{b}$	$\boldsymbol{\Gamma}_{A,T}$

The equations of motion can be represented for two modes separately, particularly horizontal and vertical one in the form of matrices. All the steps showing determination of the following matrices can be seen form Appendix B.

Vertical mode:

$$\frac{d}{dt}\begin{bmatrix} u \\ v \\ w \\ p \\ q \\ r \end{bmatrix} = \begin{bmatrix} \begin{bmatrix} rv - qw - g\sin\theta \\ pw - ru + g\cos\theta\sin\phi \\ qu - pv + g\cos\theta\cos\phi \end{bmatrix} \\ -I^{-1}\begin{bmatrix} -I_{xz}pq - I_{yz}q^2 + I_{zz}qr + I_{xy}pr - I_{yy}qr + I_{yz}r^2 \\ I_{xx}pr - I_{xy}qr - I_{xz}r^2 + I_{xz}p^2 + I_{yz}pq - I_{zz}pr \\ -I_{xy}p^2 + I_{yy}pq - I_{yz}pr - I_{xx}pq + I_{xy}q^2 + I_{xz}rq \end{bmatrix} \end{bmatrix} + \begin{bmatrix} \frac{1}{m}\begin{bmatrix} 0 \\ T_3\sin\xi \\ T_1 + T_2 + T_3\cos\xi \end{bmatrix} \\ I^{-1}\begin{bmatrix} (T_2 - T_1)l_m + T_3 l_3 \sin\xi \\ T_3 l_2 \cos\xi - (T_1 + T_2)l_1 + Q_3 \sin\xi \\ (Q_2 - Q_1) + T_3 l_2 \sin\xi + Q_3 \cos\xi \end{bmatrix} \end{bmatrix} \qquad 5.17$$

Horizontal mode:

$$\frac{d}{dt}\begin{bmatrix} u \\ v \\ w \\ p \\ q \\ r \end{bmatrix} = \begin{bmatrix} \begin{bmatrix} rv - qw - g\sin\theta \\ pw - ru + g\cos\theta\sin\phi \\ qu - pv + g\cos\theta\cos\phi \end{bmatrix} \\ -I^{-1}\begin{bmatrix} -I_{xz}pq - I_{yz}q^2 + I_{zz}qr + I_{xy}pr - I_{yy}qr + I_{yz}r^2 \\ I_{xx}pr - I_{xy}qr - I_{xz}r^2 + I_{xz}p^2 + I_{yz}pq - I_{zz}pr \\ -I_{xy}p^2 + I_{yy}pq - I_{yz}pr - I_{xx}pq + I_{xy}q^2 + I_{xz}rq \end{bmatrix} \end{bmatrix} + \begin{bmatrix} \begin{bmatrix} \frac{1}{m}\begin{bmatrix} T_1 + T_2 - D_{t_b} - D_{w_b} \\ 0 \\ L_{w_b} + L_{t_b} \end{bmatrix} \\ \begin{bmatrix} Q_2 - Q_1 \\ L_{t_b} l_t - L_{w_b} l_w \\ (T_1 - T_2) l_m \end{bmatrix} \end{bmatrix} \end{bmatrix} \qquad 5.18$$

5.2. Avionics

Avionics plays a key role in successful operation most of the modern aerial vehicles. With regard to this vehicle, it is obvious that almost everything in the UAV is under control of avionics since the vehicle is unmanned (autonomous control). The following components are the most important points, to which avionics is responsible:

- Take-off and landing;
- Horizontal flight;
- Autopilot;
- Rotor tilting;
- Vehicle rolling, pitching and yawing

In order to perform this, the flight controller is utilized, which is considered as the brain of the system. It provides a certain amount of functions that allow it to control the abovementioned points in a right way. The whole vehicle operation that starts from take-off and finishes with landing will be set by user with a help of software. This software allows user to control variety of parameters, such as altitude, geolocation of the vehicle, manures, mapping the route, and etc. [8].

The basic representation of working principle of control system for UAV is shown in Figure 5.2. Although, the real-life system is more complex, consisting of various sensors and outputs that fully controls the flight of the UAV. The most important sensors used are gyroscope, accelerometer, GPS, barometer. Accelerometer is utilized for measurement of the linear acceleration; however, there are cases when it works improperly. This implies a free fall with reading the acceleration of zero. To obtain better measurements, a gyroscope is used. This device measures the orientation of the vehicle in all three axes, which changes by pitching, rolling and yawing.

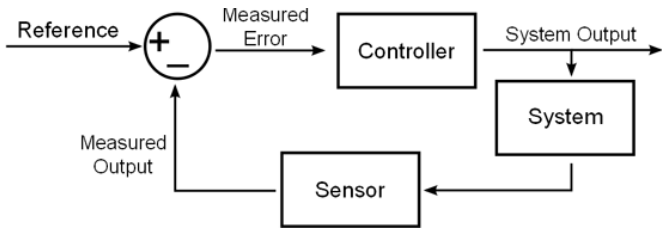

Figure 5.2. A feedback control loop [21]

5.3. PID Controller

The most widely used controller in industrial control systems is surely the PID. The reasons of this success are mainly three:

- simple structure,
- good performance for several processes,
- tunable even without a specific model of the controlled system.

The traditional PID controller consists of the addition of proportional, integral and derivative terms as shown in Figure 5.3. A PID controller continuously calculates an error value of "e" as the difference between a desired set point and a measured process variable and applies a correction based on proportional, integral, and derivative terms. The controller attempts to minimize the error over time by adjustment of a *control variable*. Due to its simplicity and abovementioned reasons, this type of controller is used for UAV' motion control.

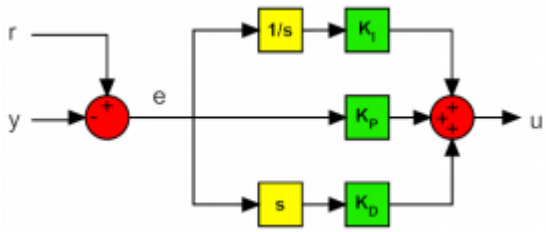

Figure 5.3. A block diagram of PID controller [6]

5.4. Control strategy

The motions of UAV could be divided into altitude, pitch, roll and yaw. Control strategies for these motions are shown in Figure5.4. Figure5.4(a) provides the altitude control, and it shows the linear correlation between motor speeds of each rotor and the altitude of the UAV. Figure5.4(b) shows the roll control, which could be done by varying the motor speeds from front two motors and constant speed of the rear motor. According to Figure 5.4(c), the pitch control can be generated by varying the rear motor' speed, while the speed of the two front motors stays the same. Regarding the yaw control, yawing moment from

reaction torque and also from the tilt angle α could successfully provide it. Tilt angle α is very useful when encountering a sudden danger of collision because by tilting the rotor, a sudden turning control would be possible [30].

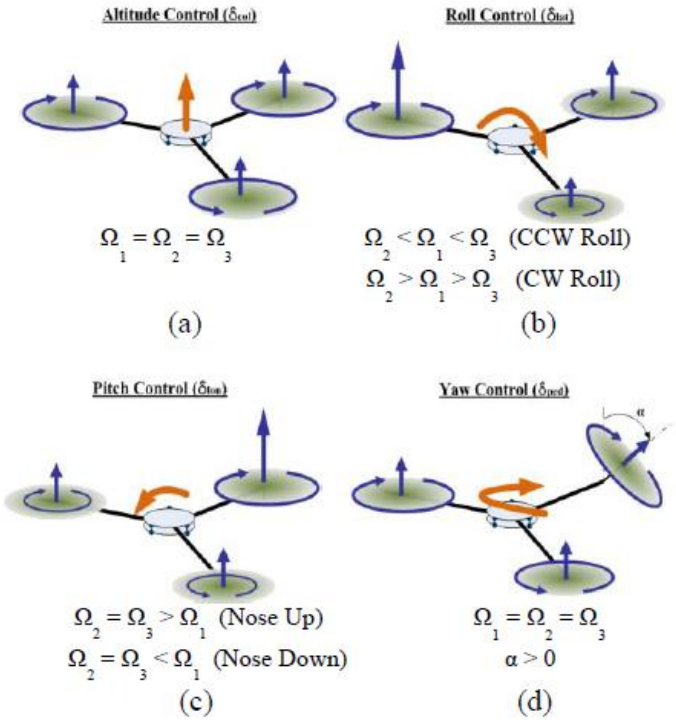

Figure 5.4. UAV Control Strategies for (a) Altitude (b) Roll (c) Pitch (d) Yaw [30]

Generally, control system for usual UAV's operations, such as vertical take-off, landing and horizontal flight can be configured quite easily based on already existing solutions. Although transition mode, which represents a motion of the UAV between horizontal and vertical flight requires coding of some special logical operations. This is due to the fact that the vehicle gains a lift force by its wings when motors stars to tilt, whereas thrust generated by these motors decreases. In order to perform a safe transition mode, both the gyroscope's and accelerometer's measurements are used to ensure that orientation and position of the UAV are right. The following control strategy can guarantee a good performance in transition mode.

As soon as a vehicle reaches a certain height, it keeps this altitude before the start of transition. Then UAV has to slightly incline upwards (pitching up) by changing the motors' rotational speeds as stated in one of the previous paragraphs. Using the information about

tilted angle and rotational speed of motors, vertical force can be calculated by a controller as well as the lift force generated by wings is to be estimated according to coded operations and coefficients for drug and lift. Furthermore, a flight controller has to change the speed of motors and tilting angle to constantly keep both the altitude and a total lift force on the same level. Simultaneous work of these processes is crucial and they are repeated till a certain moment. At that time when vehicle generates enough lift force by increase of thrust, the vertical force is not needed anymore and thus, the rotors can be tilted to 90° for further horizontal flight.

The relationships listed below show the motion of the UAV during the transition mode.

$$L = F_z(\delta) + L_w(v) \qquad 5.19$$

$$F_x(\delta) - D_w(v) = ma \qquad 5.20$$

$$F_z = (T_1 + T_2)cos\delta + T_3 \qquad 5.21$$

$$F_x = (T_1 + T_2)sin\delta \qquad 5.22$$

where L – Total lift force, F_z – vertical force by motors, δ – tilted angel, L_w – lift force generated by wings, F_x – horizontal force by motors, D_w – drug force generated by wings, m – mass, a – acceleration.

CHAPTER6. DETAILED DESIGN

Vertical Flight Mode

6.1. Motor/ESC and propeller selection

The motor selection starts from predicting the mass of the whole aircraft. The estimated mass of the aircraft is 7.5 kg. Having this information, we evaluate the total thrust needed.

$$Thrust = 2 * Total\ mass \qquad 6.1$$

$$Thrust = 2 * 7.5kg = 15kg \qquad 6.2$$

Recalling that we have three motors,

$$Thrust\ per\ mass = \frac{Thrust}{3} = 5kg \qquad 6.3$$

Now we need to select the motor with peak thrust of 5kg. Since we have an aircraft with generator, it is very important to minimize the mass and power usage of the motors. The efficiency of the RC electric motors is given by equation:

$$e = \frac{Thrust}{Power} \qquad 6.4$$

This represents how much thrust is produced per unit of power. High efficiency leads to lower power usage which leads to lower mass of an alternator and the IC engine.

Table 6.1. Performance of the T-motor U8 pro 170KV with 29*9.5CF propeller [28]

Throttle	Current, A	Power, W	Thrust, kg	Efficiency, G/W
50%	6.0	133.20	1.93	14.49
65%	11.2	248.64	3.04	12.23
75%	15.1	335.22	3.66	10.92
85%	19.5	432.90	4.33	10.00
100%	23.8	528.36	4.92	9.31

The motors were searched on the websites of high quality made motor companies, such as “Tiger motors”. As it can be seen from the Table6.1, the peak thrust is about 5kg. Also the efficiency of the motor is very high. However, the 29 inch (0.74 m) blades are quite big for

our aircraft in terms of weight, tilting capabilities and price. On the other hand, Table6.2 shows a little higher peak thrust of 5.15 kg. Even though the fact that the efficiency of the 20-inch (0.25 m) propeller is considerably lower that the efficiency of the former propeller, the matter of compactness outweighs the efficiency difference.

Table 6.2. Performance of the T-motor U8 pro 170KVwith 22*6 wood propeller [28]

Throttle, %	Current, A	Power, W	Thrust, kg	Efficiency, G/W
50%	4.40	195.35	1.85	9.47
65%	7.00	310.87	2.63	8.46
75%	9.80	435.17	3.39	7.79
85%	12.40	550.76	3.96	7.19
100%	17.31	768.66	5.15	6.7

The recommended ESC for this motor is T40A of the same Company "Tiger Motors".

6.2. IC and Generator/Starter

The maximum energy output needed from the generator is the maximum power usage during the operation. As it was mentioned before the maximum thrust needed is:

$$Thrust = 2 * Total\_mass \qquad 6.5$$

In order to obtain this thrust, all 3 motors must operate with 100% throttle. Using data from the Table 6.2, we calculate the power needed:

$$P_{total} = 3 * P_{motor,100\%throttle} \qquad 6.6$$

$$P_{total} = 3 * 768.66W = 2305.98W \qquad 6.7$$

This is the power needed to provide the maximum thrust. To estimate the generator and IC engine power rating we need to know the efficiency of energy conversion. There were no reliable sources of information about the efficiency of the brushless outrunner motor used as generator. Hence, based on the suggestion of the electrical engineering department professor, we assumed it to be 60%. From this we can get our power rating for the IC engine and generator.

$$P_{IC/alternator} = \frac{P_{total}}{0.6} = 3843W \qquad 6.8$$

In order to fit this power rating the T-Motor U11 4000 W motor was chosen as generator and 55cc (5.6HP/4170 W) IC engine as mechanical power source. In addition, this generator can also be used as starter for the engine.

Horizontal Flight Mode

6.3. Airfoil and Wing Design

6.3.1. Airfoil geometry

The figure below depicts the cross-sectional shape of a wing which is an airfoil. This part of the aircraft is responsible for lift. The lifting force is generated due to pressure difference between lower and upper surfaces. This is on account of Bernoulli's equation, which states that air speeds up over the upper surface as this has higher curvature than lower one resulting in lower pressure.

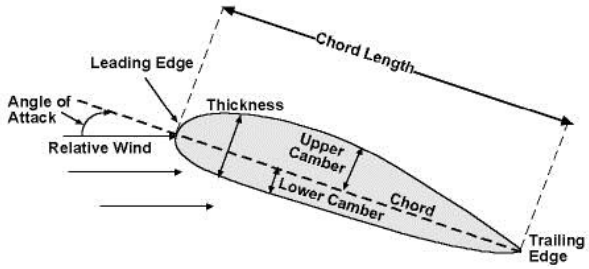

Figure 6.1. Basic parameters of an airfoil [19]

The following parameters, such as thickness to chord ratio, span, and camber percentage are crucial when the lift force needs to be determined.

6.3.2. Airfoil design

One of the most important parts of the UAV is a wing. Wing must have appropriate design characteristics in order to ensure safety flight modes. Hence, S1223 airfoil has been chosen. It has high lift and low drag coefficients for low Reynold numbers. Our UAV flights at low

velocities. Thus, airfoil was chosen according to low Reynold number with high lift and low drag characteristics. Airfoil geometry S1223 is given at Figure6.2.

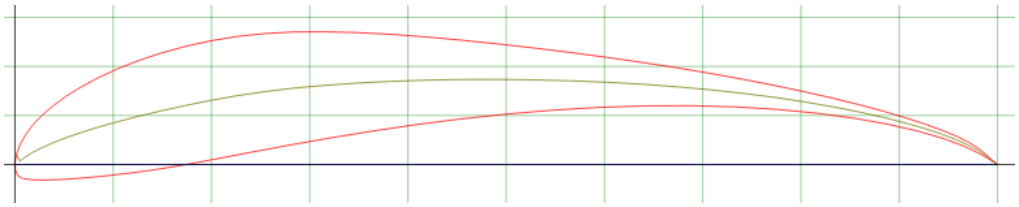

Figure 6.2. S1223 airfoil geometry [2]

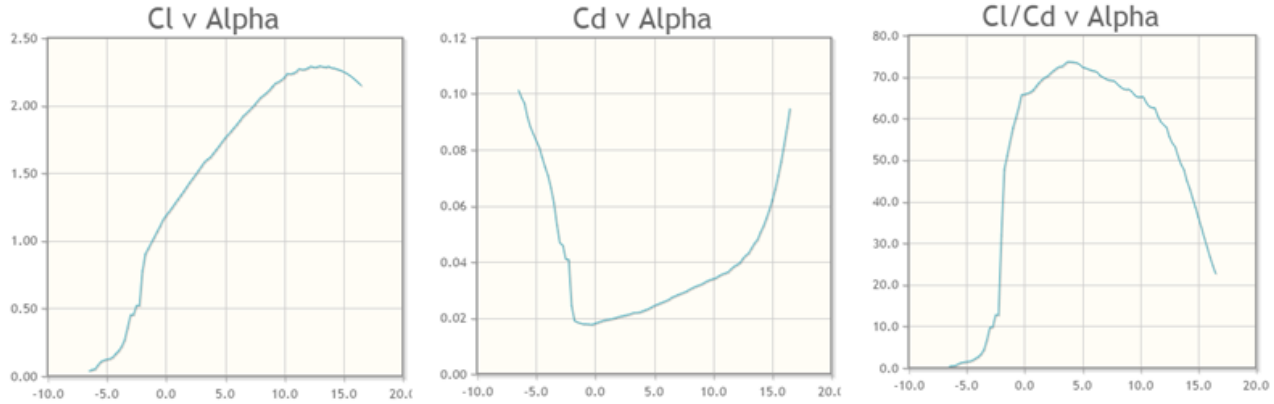

Figure 6.3. Dependence of lift/drag coefficients on angle of attack for S1223 airfoil

Figure6.3 illustrates theoretical values of the lift, drag and lift-drag ratio coefficients at different angles of attack of the S1223 airfoil. Angle of 2.5° alpha has been identified as the most efficient one for our case. At this angle airfoil has the least drag and medium lift. Also, it is possible to increase an angle of attack, which maximizes the lift coefficient. However, at greater angles of attack a drag is added. Therefore, angle of attack has been chosen according to maximum lift and drag coefficient. This concept accepted to be most efficient and values are given in the Table6.3.

Table 6.3. Airfoil characteristics at Re=200 000 [1]

alpha	C_L	C_D
2.500	1.4884	0.02083

In order to apply lift and drag characteristics given at the Table6.3 our designed wing must operate at the same Reynolds number. First step is to identify chord length of the airfoil.

$$Re = \frac{\rho * v * c}{\mu} \qquad 6.9$$

Table 6.4. Values for calculation of a chord length

Re	Velocity, v	Density, ρ	Temperature, T	Dynamic viscosity, μ
200000	15 m/s	1.2 kg/m^3	300 K	1.846*10^{-5} kg/m*s

All required parameters for calculation are given in the table above. According to [12], the chord length of the airfoil has been identified: *c=200 mm*. The location of cord is represented in the Figure6.3.

6.3.3. Wingspan

As the chord length is identified, the next step is to calculate span of the wing. Hence, the lift force equation can be used:

$$F_L = \frac{1}{2} * C_L * A * \rho * v^2 \qquad 6.10$$

$$F_L = \frac{1}{2} * C_L * c * L * \rho * v^2 \qquad 6.11$$

According to design specifications our UAV, its mass is equal to 7.5 kg. Hence, the minimum lift force is F_L=75 N and C_L=1.4884 as given at the Table6.3. Other required parameters to define a wingspan are given at the Table6.4. Thus, the minimum value of wingspan length is L=1.87 m. Preliminary wing requirements are *2.0 m of wingspan and 0.20 m of chord length*.

6.3.4. Airfoil Simulation

Ansys software, particularly its simulation feature has been used for validation of the results identified for both airfoil and wing. Simulation parameters were set according to all theoretical design specification identified in the previous section. Before a start of the simulation, mesh validation has been made to run the simulation properly. Also, mesh verification is made to ensure that results of simulation are applicable for the real life applications. Tetrahedron mesh type was used during flow analysis on airfoil. Figure 6.4 illustrates the size of mesh around airfoil. Simulation was done in a way that boundary conditions in a wind tunnel were imitated. Mesh is coarse around the airfoil in order to

obtain accurate results. Mesh dimensions were decreased until the results of the simulation reached convergence and negligible error. Total number of nodes of mesh is 187850.

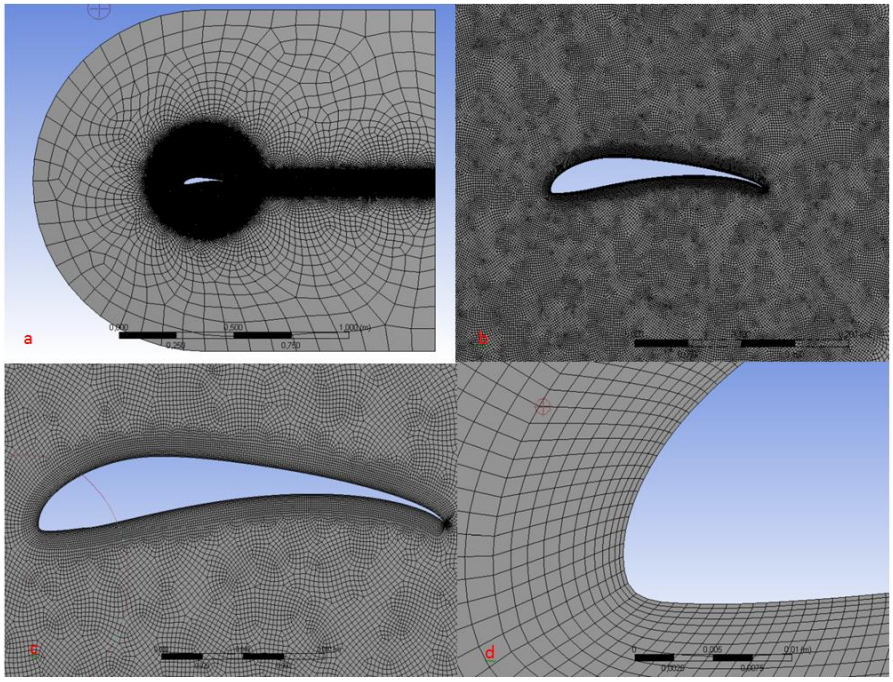

Figure 6.4. Mesh Verification, a) wind tunnel, b) and c) mesh around airfoil, d) mesh near the boundary layer

The number of simulations made was three. This is on account of finding best design parameters for the wing to obtain a better performance of the UAV. The results of these simulations are presented in the Table6.5 below. According to it, a generated lift force is not enough for the first and the second cases, since its magnitude is less than the minimum required one (75 N) for the cruise regime. Hence, additional simulation has been made to find out appropriate design parameters of the airfoil and the wing. Based on data from the same table, increase in a chord length resulted in a significant increase of total lift of the wing. As a result, wing configuration with a desired lift of 75 N was obtained.

Table 6.5. Results of the simulation of S1223 wing for different parameters

angle of attack =2.5, chord length= 0.2 m		angle of attack =3.0, chord length= 0.2 m		angle of attack =2.5, chord length= 0.22 m	
Simulation #1		Simulation #2		Simulation #3	
Velocity, m/s	15	Velocity, m/s	15	Velocity, m/s	15
Width, m	2.0	Width, mm	2000	Width, mm	2000
Drag, N	3.2	Drag, N	3.6	Drag, N	4
Lift, N	69.2	Lift, N	71.7	Lift, N	75

Results of velocity and pressure distribution contour around the airfoil are shown in Figures6.5-6.6. These airfoil specifications are considered to be appropriate for the UAV design requirements.

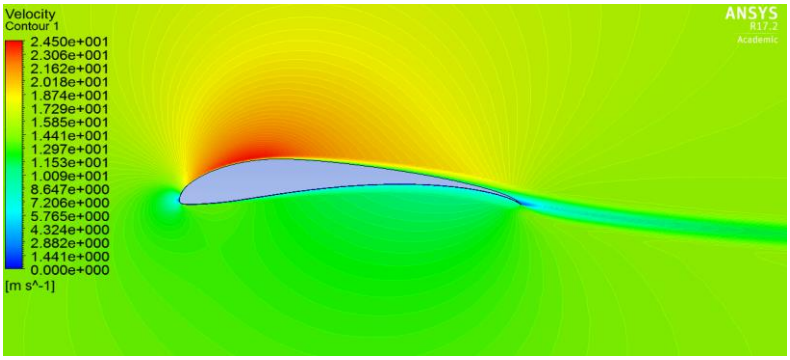

Figure 6.5. Velocity distribution for the S1223 wing

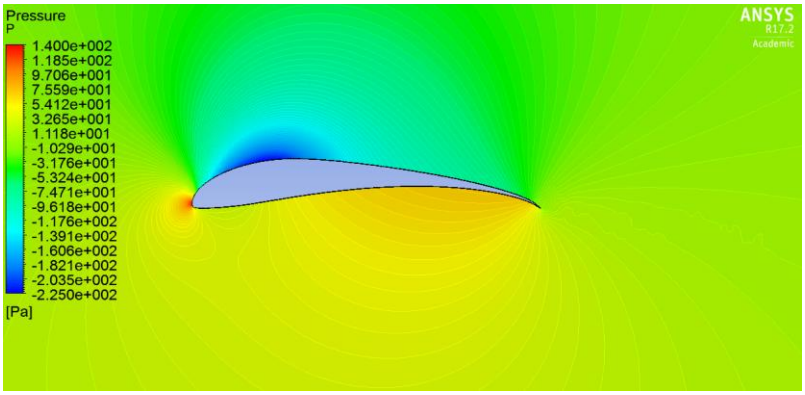

Figure 6.6. Pressure contour for the S1223 wing

6.4. Stabilizer Simulation

Neutral Airfoil is a rear wing of the UAV and its works as a stabilizer. It produces insignificant lift and drag forces. Hence, it is called neutral and NACA0012 airfoil was chosen for this purpose in the project (figure). Table6.6 shows the results of airfoil simulation and wing specifications.

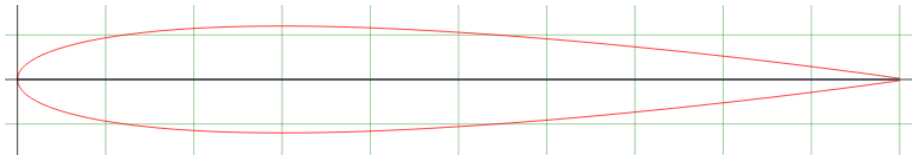

Figure 6.7. NACA0012 Airfoil geometry [2]

Table 6.6. NACA0012 Stabilizer characteristics

Airfoil	NACA0012
Velocity, m/s	15
Angle of attack, degrees	0
Chord length, m	0.10
Width, m	0.70
Drag, N	0.80
Lift, N	0.65

6.5. Fuselage Simulation

In order to know the total life and total drag of the proposed design, a fuselage simulation was conducted. This simulation on Ansys was made with the use of symmetry function, when only half part of the fuselage was analyzed. Symmetry function gave an opportunity to obtain quick results of full fuselage drag and lift magnitude.

The results of this simulation are provided in Table6.7 and Figures6.8-6.9. Negative sign on lift force will results in total lift decrease (table). However, its magnitude is insignificant in our case. Velocity and pressure contour profiles are presented on figure x and x.

Table 6.7. Fuselage characteristics

Angle of attack, degrees	0
Velocity, m/s	15
Drag, N	3.60
Lift, N	-0.04

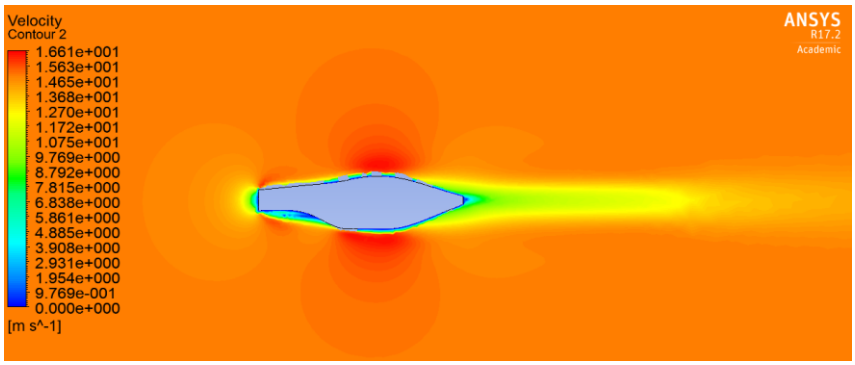

Figure 6.8. Velocity distribution for the fuselage

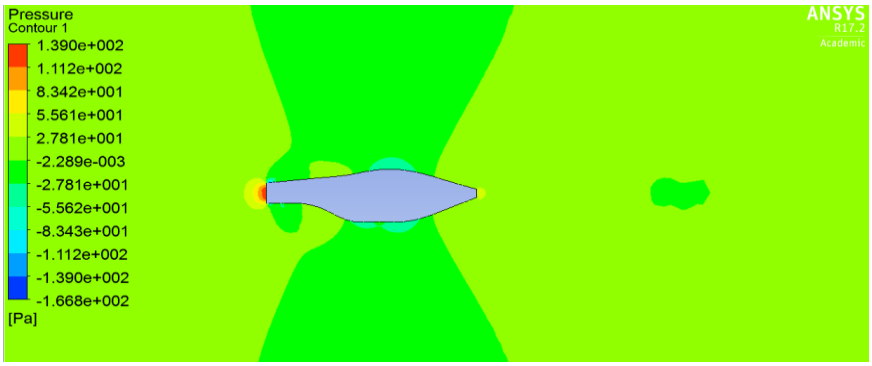

Figure 6.9. Pressure contour for the fuselage

Final preliminary values of total drag and total lift of designed UAV parameters are shows in the |Table6.8. They are calculated by summation of drag and lift coefficients of front and rear wings and double fuselage. These values are important to choose appropriate motors and IC engine.

Table 6.8. UAV total drag and total lift characteristics

Velocity, m/s	15
Total lift, N	90.6
Total drag, N	12.0

6.6. Battery

The battery capacity can be calculated based on the endurance limit. The endurance which is the time the UAV can cruise comprises two hours. The power usage of all the motors can be calculated from the thrust needed to sustain the cruise speed and the efficiency of the motor. In order to extrapolate the efficiency of the motor the efficiency curve was made based on the data from Table6.2.

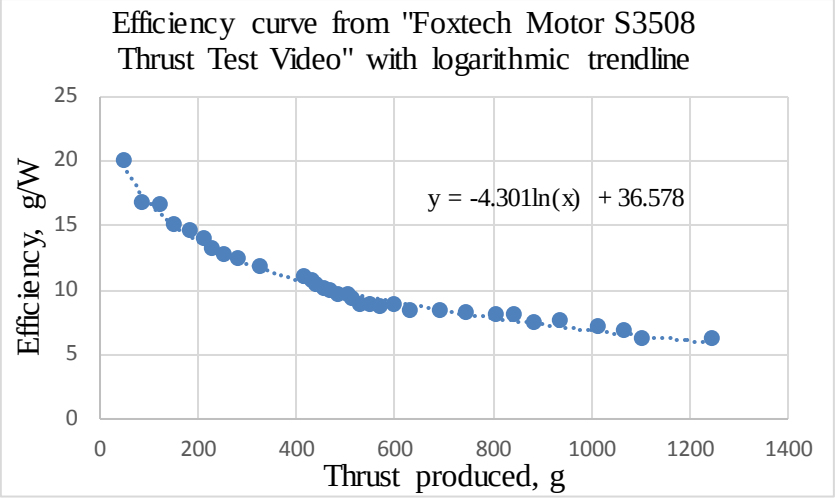

Figure 6.10. Graph of the efficiency of the S3508 motor [13]

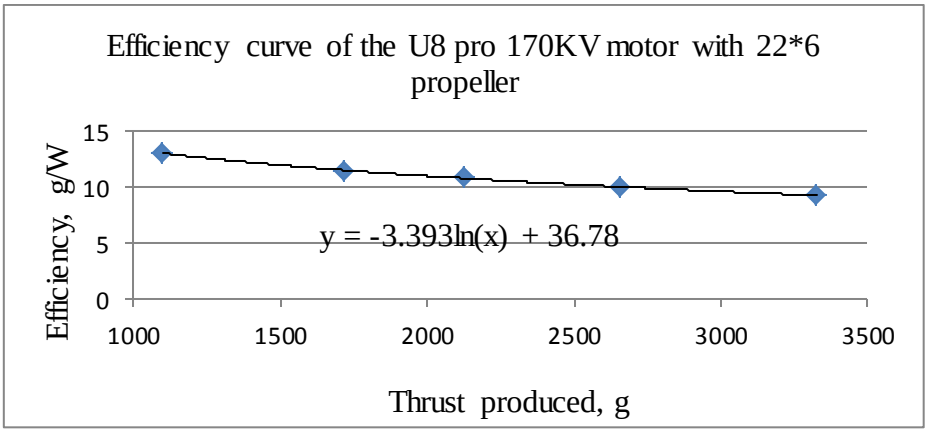

Figure 6.11. Graph of the efficiency of the U8 motor with extrapolated data for 44.4 V

$$T_{cruise} = \frac{Total\ drag}{g} = \frac{12}{9.81} \approx 1.20kg \qquad 6.12$$

The cruise needed for each motor is

$$T_{cruisepermotor} = \frac{T_{cruise}}{2} = 0.60kg \qquad 6.13$$

Using Figure6.12 and applying 0.60kg on the x axis we obtain the efficiency of 15.08 g/watt. This leads to 39.79W usage per motor, which comprises 80W for $P_{total,cruise}$. Thus the capacity needed is:

$$C = Endurance * \frac{P_{total,cruise}}{(e_{battery} * e_{usage})} = 1.5h * \frac{80W}{0.8*0.9} = 167Wh \qquad 6.14$$

Since the motor works on 12S (44.4V) battery, the battery specification would be:

$$\frac{C}{V} = A * h = \frac{167}{44.4} = 3754mAh \qquad 6.15$$

Therefore, the battery of 12S and 3200mAh or more for enhanced endurance is needed.

6.7. Servo motor

A servo motor which is normally a simple DC motor is used in this project for specific angular rotation of the motors with propellers with a help of additional servomechanism. Its characteristics have to be chosen correctly to ensure that it could rotate the rotor. For this particular case, Turnigy™ TGY-306G-HV Ultra Fast servomotor with the mass of 21g and 3.7kg*cm torque working on 7.2V was used. Calculations of needed torque are presented below. The Figure6.12 depicts 3D model of the propeller tilt mechanism drawn in Solidworks.

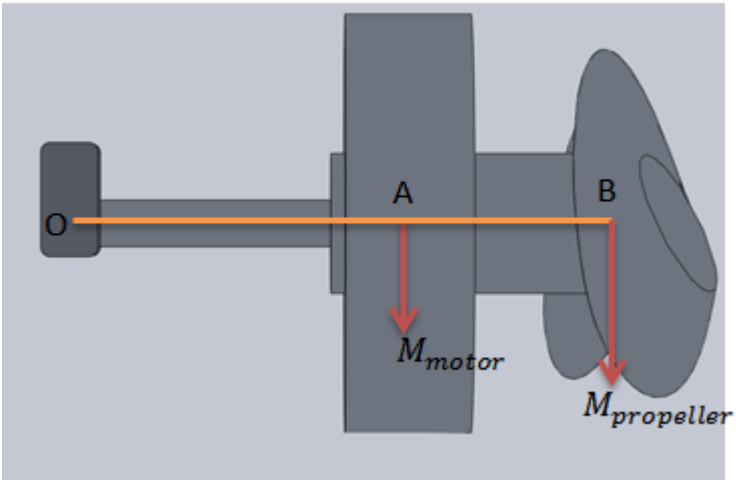

Figure 6.12. Tilting mechanism for the rotor

$$\sum \tau_O = M_{motor} * \overline{OA} + M_{propeller} * \overline{OB} = 0.240kg * 70cm + 0.100kg * 95cm = 2.63kg * cm \qquad 6.16$$

where M_{motor} is the motor mass, $\overline{OA}$ is a distance between centers of motor and servomotor, $M_{propeller}$ is the propeller's mass and $\overline{OB}$ is a distance between centers of propeller and servomotor [14].

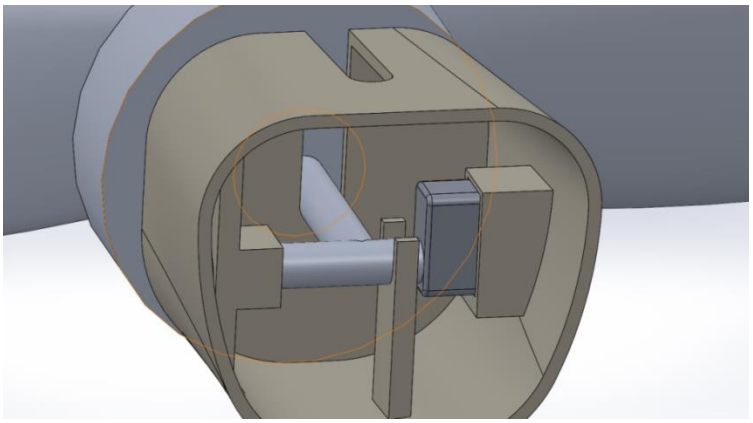

Figure 6.13. 3D model of the propeller tilt mechanism

6.8. 3D view of the design model

The 3D view of the model is shown below in the Figure 6.14. Appendix C contains other detailed pictures of the UAV model created in SolidWorks.

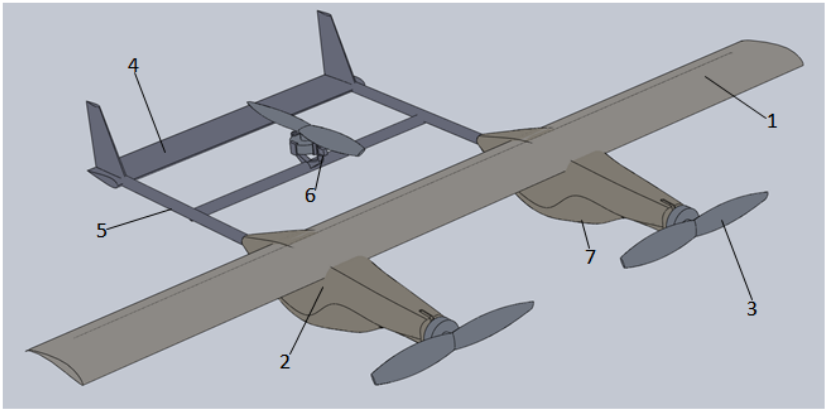

1 – wing, 2 – fuselage, 3 – motor with propeller, 4 – stabilizer, 5 – fiber tubes, 6 – servo motor, 7 – payload camera

Figure 6.14. 3D model of the UAV final design

6.9. Manufacturing

Ease of manufacturing is one of the key factors identifying an overall cost of a UAV. Reduction of manufacturing costs could be reached by using enhanced integrated components. Utilization of modern techniques could reduce per-unit costs of the UAV. Reducing energy consumption and autonomous production regimes without physical labor will further decrease cost of manufacturing, which results in operational cost reduction.

UAVs with the lowest per-unit cost and lower operating cost are usually chosen to ensure financial superiority [11].

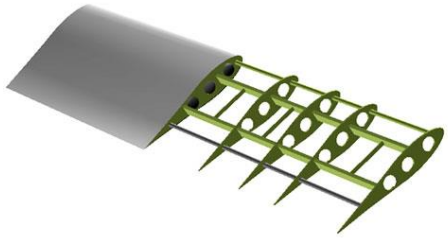

Figure 6.15. Wing skeleton [11]

Each airfoil can be made separately and connected with each other as it can be seen at figure6.15. Airfoil can be easily cut with 5-Axis CNC Milling Machine. After connecting all parts the structure can be covered by wood-sheet or thin plastic. Airfoil and connecting materials are of wood to minimize the weight [16].

Fuselage model can be made from foam and then covered by epoxy glass. Several layers of epoxy glass should be applied and after each layer there is a time for shape to be ready for the addition of the next layer. When shape will be ready, foam will be removed from the fuselage [15]. Figure6.16 illustrates how similar aircraft fuselage has been made.

Figure 6.16. Hot-wired foam blocks shaping [16]

Connection between wings and fuselages are made through screw connections. With regard to the tubes at the rear part of the UAV, connections are made of glue, pressing or fusing.

CHAPTER7. CONCLUSION

This capstone project report has discussed the design of the small-scale UAV with the main aim of performing different tasks during horizontal and vertical flights. This work included analysis of the different design alternatives, selection of the best option for the listed objectives, discussion on propulsion systems and estimation of the total take-off mass. In addition, detailed design provided practical calculations and estimations for an optimal part selection, such as choosing of motor with an appropriate propeller, battery, IC engine and airfoil geometry. The complete model of the UAV, containing its wings, tail, fuselage was developed based on detailed calculations provided.

The CAD model that was built in Solidworks represents practical dimensions, and it was used further to obtain simulation results on various parameter functions. The outcomes of the simulations influenced the overall design of both airfoil and fuselage. Furthermore, the lab work conditions have been designed in order to perform the experimental analysis of the engine and alternator for an identification of their working parameters and efficiency. Finally, the prototype's behavior in real-life conditions has to be investigated and this requires the future studies.

REFERENCES

[1] Airfoiltools.com. S1223 (s1223-il) Xfoil prediction polar at RE=200,000. http://airfoiltools.com/polar/details?polar=xf-s1223-il-200000 (Accesssed 12th November 2016)

[2] Airfoiltools.com. S1223 high lift low Reynolds number airfoil. http://airfoiltools.com/airfoil/details?airfoil=s1223-il. (Accessed 12th November 2016)

[3] Austin. R. (2010). Unmanned Aircraft Systems.[Sl].

[4] Bayliss. J.. 2013. Unmanned Aerial Vehicle 100% Report.

[5] Bemil.chosun.com. Double fuselage aircrafts during WW2. http://bemil.chosun.com/nbrd/bbs/view.html?b_bbs_id=10044&pn=0&num=14781(Accessed 13th November 2016)

[6] Bresciani, T. (2008). Modelling, identification and control of a quadrotor helicopter. *MSc Theses*.

[7] Çetinsoy. E.. Dikyar. S.. Hançer. C.. Oner. K. T.. Sirimoglu. E.. Unel. M.. & Aksit. M. F. (2012). Design and construction of a novel quad tilt-wing UAV. Mechatronics. 22(6). 723-745.

[8] Collinson, R. P. G. (2003). Fly-by-wire flight control. In *Introduction to Avionics Systems* (pp. 159-224). Springer US.

[9] Dalamagkidis. K. (2015). Classification of UAVs. In Handbook of Unmanned Aerial Vehicles (pp. 83-91). Springer Netherlands.

[10] Eide, Arvid R., Roland Jenison, Larry Northup, and Steven Mickelson. Engineering fundamentals and problem solving. McGraw-Hill, 2008.

[11] Flynn, Eric P. "Low-cost approaches to uav design using advanced manufacturing techniques." In *Integrated STEM Education Conference (ISEC), 2013 IEEE*, pp. 1-4. IEEE, 2013.

[12] Gundlach. J. (2012). Designing unmanned aircraft systems: A comprehensive approach. American Institute of Aeronautics and Astronautics.

[13] Helicopter Flying Handbook. 2017. United State Department of Transportation. https://www.faa.gov/regulations_policies/handbooks_manuals/aviation/helicopter_flying_handbook/media/hfh_ch02.pdf (Last modified 23rd March 2017).

[14] Hobbyking.com. 2016. Turnigy™ TGY-306G-HV Ultra Fast/High Torque. https://hobbyking.com/en_us/turnigytm-tgy-306g-hv-ultra-fast-high-torque-ds-mg-hv-alloy-case-3-7kg-0-05sec-21g.html (Accessed 24th November 2016)

[15]http://www.mfhb.org.nz/joomla/index.php?option=com_content&view=article&id=115:sukhoi-mk-3-build&catid=40:general-articles

[16] http://www.motisvirtualjetdesign.com/FLIGHTLINE.htm

[17] Jaeger. M., Adair. D. (2016). Conceptual Design of a High-Endurance Hybrid Electric Unmanned Aerial Vehicle. 4th International Conference on Nanomaterials and Advanced Energy Storage Systems (INESS).

[18] Lieh. J.. Spahr. E.. Behbahani. A. and Hoying. J.. 2011 Design of hybrid propulsion systems for unmanned aerial vehicles. In 17th AIAA International Space Planes and Hypersonic Systems and Technologies Conference.

[19] Macheret. J.. Teichman. J.. & Kraig. R. (2011). Conceptual Design of Low-Signature High-Endurance Hybrid-Electric UAV. IDA.. Virginia. IDA Doc.. NS D-4496.

[20] Pahl, Gerhard, and Wolfgang Beitz. Engineering design: a systematic approach. Springer Science & Business Media, 2013.

[21] Project thermoelectric cooler controller system. http://nasa.olin.edu/projects/2010/tec/work_introCT.htm (Accessed 15th February 2017).

[22] Robotshop. How to make a Drone/UAV Lesson 3: propulsion. http://www.robotshop.com/blog/en/make-uav-lesson-3-propulsion-14785. (Accessed 11th November 2016

[23] Ryll. M.. Bülthoff. H. H.. & Giordano. P. R. (2012. May). Modeling and control of a quadrotor UAV with tilting propellers. In Robotics and Automation (ICRA). 2012 IEEE International Conference on (pp. 4606-4613). IEEE.

[24] Saeed. A. S.. Younes. A. B.. Islam. S.. Dias. J.. Seneviratne. L.. & Cai. G. (2015. June). A review on the platform design. dynamic modeling and control of hybrid UAVs. In Unmanned Aircraft Systems (ICUAS). 2015 International Conference on (pp. 806-815). IEEE.

[25] Schömann. J. (2014). Hybrid-electric propulsion systems for small unmanned aircraft (Doctoral dissertation. Technische Universität München).

[26] Shampanier, M. /8th grade – Aerodynamics. http://www.portnet.k12.ny.us/Page/7890. (Accessed 16th November 2016)

[27] Tayal, S. P. "Engineering design process." International Journal of Computer Science and Communication Engineering (2013): 1-5.

[28] T-motor. T-motor U7 power type brushless outrunner. http://www.rctigermotor.com/html/2013/Power-Type_0928/92.html. (Accessed 11th November 2016)

[29] Wikipedia. "Aircraft principal axes". Last Modified 9 November 2016. https://en.wikipedia.org/wiki/Aircraft_principal_axes

[30] Yoo, D. W., Oh, H. D., Won, D. Y., & Tahk, M. J. (2010, June). Dynamic modeling and control system design for Tri-Rotor UAV. In *Systems and Control in Aeronautics and Astronautics (ISSCAA), 2010 3rd International Symposium on* (pp. 762-767). IEEE

[31] Youtube. Foxtech Motor S3508 Thrust Test Video. https://www.youtube.com/watch?v=maisALyuINo. (Accessed 10th November 2016)

APPENDICES

Appendix A. Experiment related material

1) Code for Arduino

```
#include <Servo.h>
Servo yservo; Servo xservo; // servos for x and y
//set initial values for x and y
int ypos = 0;
int xpos= 0;
void setup(){
  xservo.attach(14); //(analog pin 0) for the x servo
  yservo.attach(9); //(pwm pin) for the y server
   Serial.begin(19200);  // 19200 is the rate of communication
  Serial.println("Rolling");  // some output for debug purposes.
 }
void loop() {
  static int v = 0; // value to be sent to the servo (0-180)
  if ( Serial.available())  {
    char ch = Serial.read();  // read in a character from the serial port and assign to ch
    switch(ch) { // switch based on the value of ch
      case '0'...'9':  // if it's numeric
        v = v * 10 + ch - '0';
        /*
          so if the chars sent are 45x (turn x servo to 45 degs)..
          v is the value we want to send to the servo and it is currently 0
          The first char (ch) is 4 so
          0*10 = 0 + 4 - 0 = 4;
          Second char is 4;
```

```
        4*10 = 40 + 5 = 45 - 0 = 45;
        Third char is not a number(0-9) so we drop through...
      */
       break;
     case 'x': // if it's x
     /*
      ....and land here
      where we send the value of v which is now 45 to the x servo
      and then reset v to 0
     */
       xservo.write(v);
       v = 0;
       break;
     case 'y':
       yservo.write(v);
       v = 0;
       break;
  } } }
```

2) Code for Processing:

```
import processing.serial.*;
int xpos=90; // set x servo's value to mid point (0-180);
int ypos=90; // and the same here
Serial port; // The serial port we will be using
void setup()
{
  size(360, 360);
```

```
 frameRate(100);
 println(Serial.list()); // List COM-ports
 //select second com-port from the list (COM3 for my device)
 // You will want to change the [1] to select the correct device
 // Remember the list starts at [0] for the first option.
 port = new Serial(this, Serial.list()[0], 19200);
}
void draw()
{
 fill(175);
 rect(0,0,360,360);
 fill(255,0,0); //rgb value so RED
 rect(180, 175, mouseX-180, 10); //xpos, ypos, width, height
 fill(0,255,0); // and GREEN
 rect(175, 180, 10, mouseY-180);
 update(mouseX, mouseY);
}
void update(int x, int y)
{
 //Calculate servo postion from mouseX
 if (mousePressed){
  ypos=100;
 } else {
 xpos= x/2;
 ypos = y/2;
 }
 //Output the servo position ( from 0 to 180)
 port.write(xpos+"x");
```

```
 port.write(ypos+"y");
}
```

3) Pictures of the laboratory setup

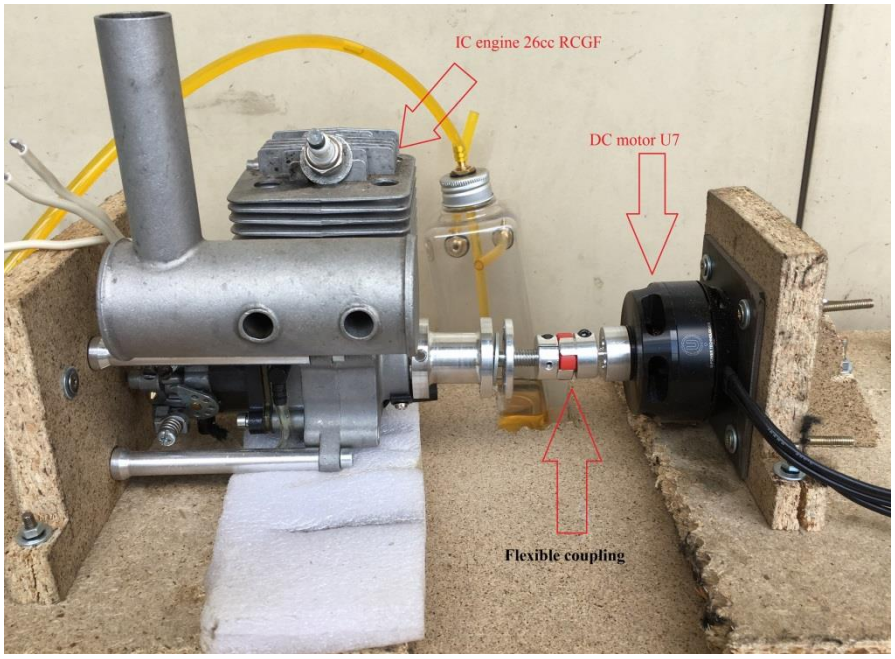

Figure A1. IC engine and DC motor connection

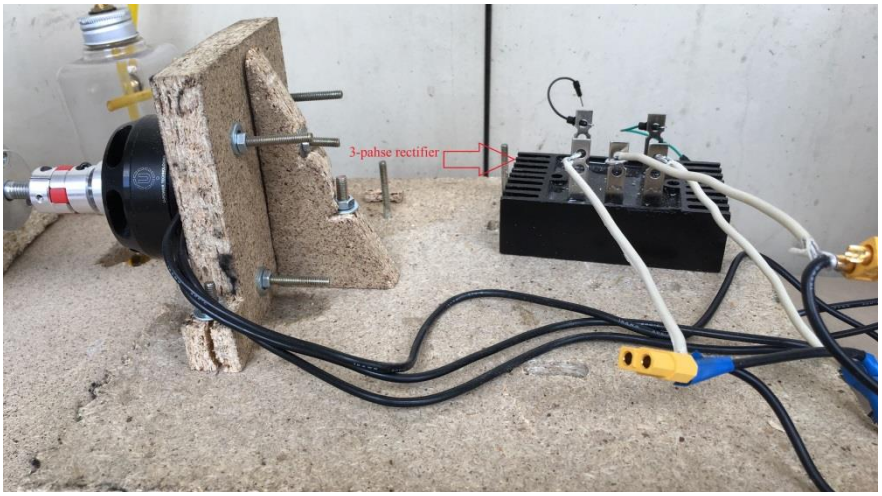

Figure A2. 3-phase rectifier connection

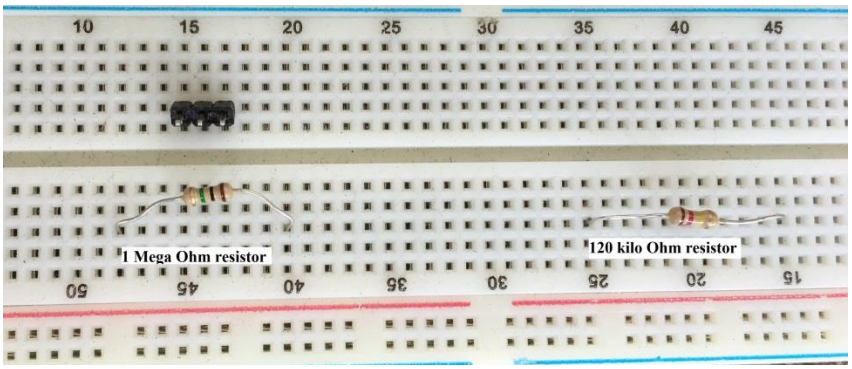

Figure A3. Resistors on breadboard

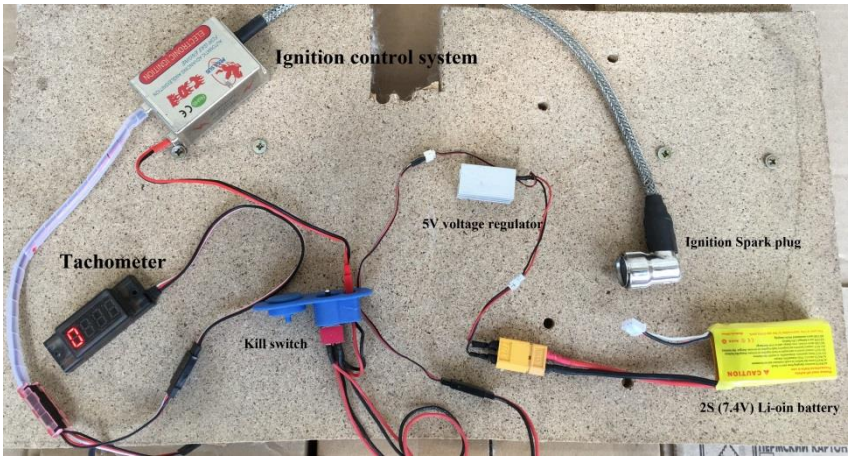

Figure A4. Ignition and tachometer wiring

Appendix B. Mathematical modeling

$$L_{t_b} = \frac{1}{2} * \rho * C_{L_t} * A_t * V_{in}{}^2$$

$$L_{w_b} = \frac{1}{2} * \rho * C_{L_w} * A_w * V_{in}{}^2$$

$$D_{t_b} = \frac{1}{2} * \rho * C_{D_t} * A_t * V_{in}{}^2$$

$$D_{w_b} = \frac{1}{2} * \rho * C_{D_w} * A_w * V_{in}{}^2$$

$V_{in} = \sqrt{V^2 + \frac{2*T}{\rho * A_m}}$, where

A_t is the are of the stabilizer, A_w is the are of the wing, A_m is the are of the motor, $C_{L_t}, C_{L_w}, C_{D_t}, C_{D_w}$ are lift and drag coefficients for stabilizer and wing respectively,

V_{in} is the velocity of the UAV and V is the velocity of the motor

Translational kinematics:

Considering the translational motion of the aircraft, this is direct transformation changing linear velocities (u, v, w), from F_B into F_V

$$\begin{bmatrix} \dot{x_e} \\ \dot{y_e} \\ \dot{z_e} \end{bmatrix} = R \begin{bmatrix} u \\ v \\ w \end{bmatrix}.$$

$$\begin{bmatrix} \dot{x_e} \\ \dot{y_e} \\ \dot{z_e} \end{bmatrix} = \begin{bmatrix} cos\Theta cos\psi & sin\phi sin\Theta cos\psi - cos\phi sin\psi & cos\phi sin\Theta cos\psi + sin\phi sin\psi \\ cos\Theta sin\psi & sin\phi sin\Theta sin\psi + cos\phi sin\psi & cos\phi sin\Theta sin\psi - sin\phi cos\psi \\ -sin\Theta & sin\phi cos\Theta & cos\phi cos\Theta \end{bmatrix} \begin{bmatrix} u \\ v \\ w \end{bmatrix}$$

Rotational kinematics:

$$\boldsymbol{\theta} = [\phi \quad \theta \quad \psi]^T$$

This transformation is obtained by sequential transformation of axes and angular velocities,

$$\begin{bmatrix} \dot{\phi} \\ \dot{\Theta} \\ \dot{\psi} \end{bmatrix} = \begin{bmatrix} 1 & sin\phi tan\Theta & cos\phi tan\Theta \\ 0 & cos\phi & -sin\phi \\ 0 & sin\phi sec\Theta & cos\phi sec\Theta \end{bmatrix} \begin{bmatrix} p \\ q \\ r \end{bmatrix}$$

Translational dynamics:

Considering that the mass of the aircraft is constant, the state variables related to translational dynamics can be calculated according to Newton's Second Law: the summation of all external forces acting on a rigid body is equal to the time rate of change of the linear momentum of the body. This is shown by eqn (22)

$$\begin{bmatrix} \dot{u} \\ \dot{v} \\ \dot{w} \end{bmatrix} = \begin{bmatrix} cos\Theta cos\psi & sin\phi sin\Theta cos\psi - cos\phi sin\psi & cos\phi sin\Theta cos\psi + sin\phi sin\psi \\ cos\Theta sin\psi & sin\phi sin\Theta sin\psi + cos\phi sin\psi & cos\phi sin\Theta sin\psi - sin\phi cos\psi \\ -sin\Theta & sin\phi cos\Theta & cos\phi cos\Theta \end{bmatrix}^T \begin{bmatrix} 0 \\ 0 \\ g \end{bmatrix} + \frac{1}{m} \boldsymbol{F}_{A,T}^b - \begin{bmatrix} p \\ q \\ r \end{bmatrix} \times \begin{bmatrix} u \\ v \\ w \end{bmatrix}$$

$$\boldsymbol{F}_{A,T}^b = \begin{bmatrix} \boldsymbol{F}_{A,T_x}^b \\ \boldsymbol{F}_{A,T_y}^b \\ \boldsymbol{F}_{A,T_z}^b \end{bmatrix}$$

After performing some calculations and leaving the derivatives of the state variables alone at the left side, we obtain

$$\begin{bmatrix}\dot{u}\\ \dot{v}\\ \dot{w}\end{bmatrix}=\begin{bmatrix} rv-qw-gsin\Theta+\dfrac{\boldsymbol{F}^{b}_{A,T_x}}{m}\\ pw-ru+gcos\Theta sin\phi+\dfrac{\boldsymbol{F}^{b}_{A,T_y}}{m}\\ qu-pv+gcos\Theta cos\phi+\dfrac{\boldsymbol{F}^{b}_{A,T_z}}{m}\end{bmatrix}$$

Rotational dynamics:

Applying Euler's formula; the summation of the external moments acting on a rigid body is equal to the time rate of change of the angular momentum,

$I\begin{bmatrix}\dot{p}\\ \dot{q}\\ \dot{r}\end{bmatrix}=-\begin{bmatrix}p\\ q\\ r\end{bmatrix}\times\left(I\begin{bmatrix}p\\ q\\ r\end{bmatrix}\right)+\begin{bmatrix}\boldsymbol{\Gamma}_{A,T_x}\\ \boldsymbol{\Gamma}_{A,T_y}\\ \boldsymbol{\Gamma}_{A,T_z}\end{bmatrix}$, or this can be re-written as

$$\begin{bmatrix}\dot{p}\\ \dot{q}\\ \dot{r}\end{bmatrix}=-I^{-1}\begin{bmatrix}p\\ q\\ r\end{bmatrix}\times\left(I\begin{bmatrix}p\\ q\\ r\end{bmatrix}\right)+I^{-1}\begin{bmatrix}\boldsymbol{\Gamma}_{A,T_x}\\ \boldsymbol{\Gamma}_{A,T_y}\\ \boldsymbol{\Gamma}_{A,T_z}\end{bmatrix}$$

$I=\begin{bmatrix}I_{xx} & I_{xy} & I_{xz}\\ I_{yx} & I_{yy} & I_{yz}\\ I_{zx} & I_{zy} & I_{zz}\end{bmatrix}$, $I_{xy}=I_{yx}$, $I_{xz}=I_{zx}$, $I_{yz}=I_{zy}$

So after consecutive calculations;

$$\begin{bmatrix}\dot{\boldsymbol{p}}\\ \dot{\boldsymbol{q}}\\ \dot{\boldsymbol{r}}\end{bmatrix}=-\boldsymbol{I^{-1}}\begin{bmatrix}-\boldsymbol{I_{xz}pq}-\boldsymbol{I_{yz}q^2}+\boldsymbol{I_{zz}qr}+\boldsymbol{I_{xy}pr}-\boldsymbol{I_{yy}qr}+\boldsymbol{I_{yz}r^2}\\ \boldsymbol{I_{xx}pr}-\boldsymbol{I_{xy}qr}-\boldsymbol{I_{xz}r^2}+\boldsymbol{I_{xz}p^2}+\boldsymbol{I_{yz}pq}-\boldsymbol{I_{zz}pr}\\ -\boldsymbol{I_{xy}p^2}+\boldsymbol{I_{yy}pq}-\boldsymbol{I_{yz}pr}-\boldsymbol{I_{xx}pq}+\boldsymbol{I_{xy}q^2}+\boldsymbol{I_{xz}rq}\end{bmatrix}+\boldsymbol{I^{-1}}\begin{bmatrix}\boldsymbol{\Gamma}_{A,T_x}\\ \boldsymbol{\Gamma}_{A,T_y}\\ \boldsymbol{\Gamma}_{A,T_z}\end{bmatrix}$$

Appendix C. 3D modeling design

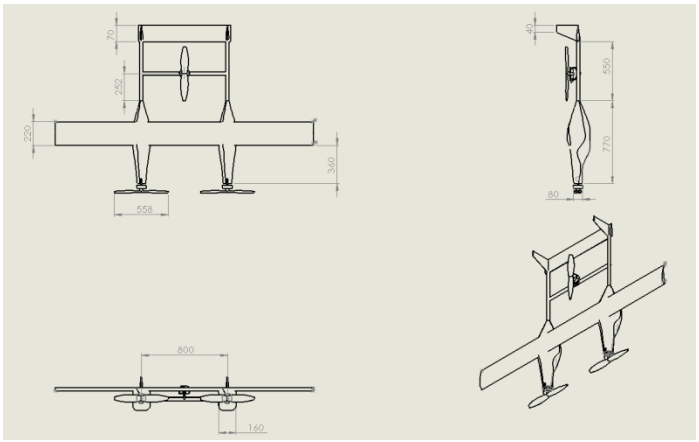

Figure C1. CAD drawing

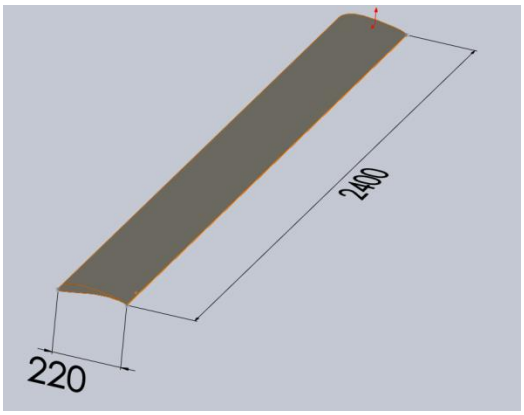

Figure C2. Wing specifications

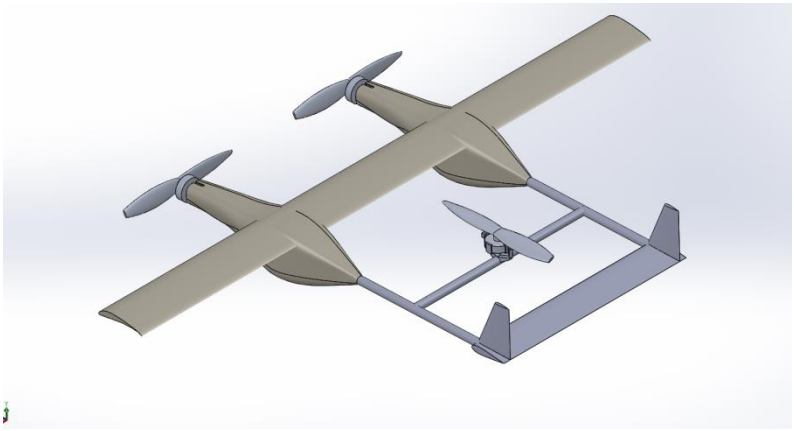
Figure C3. Horizontal flight

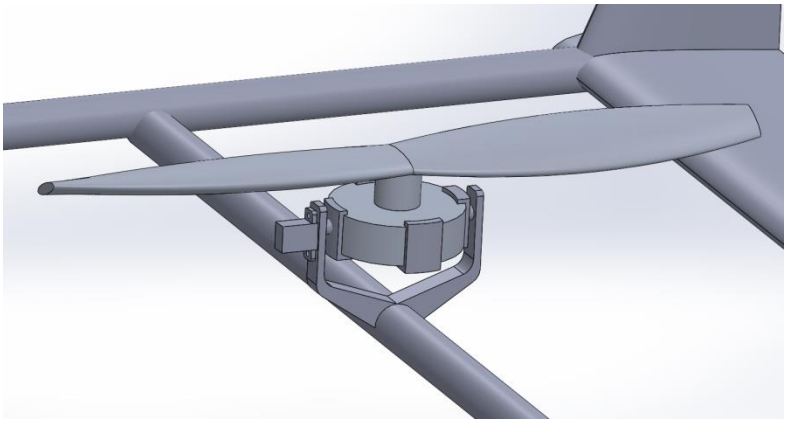
Figure C4. Rear tilt rotor mechanism

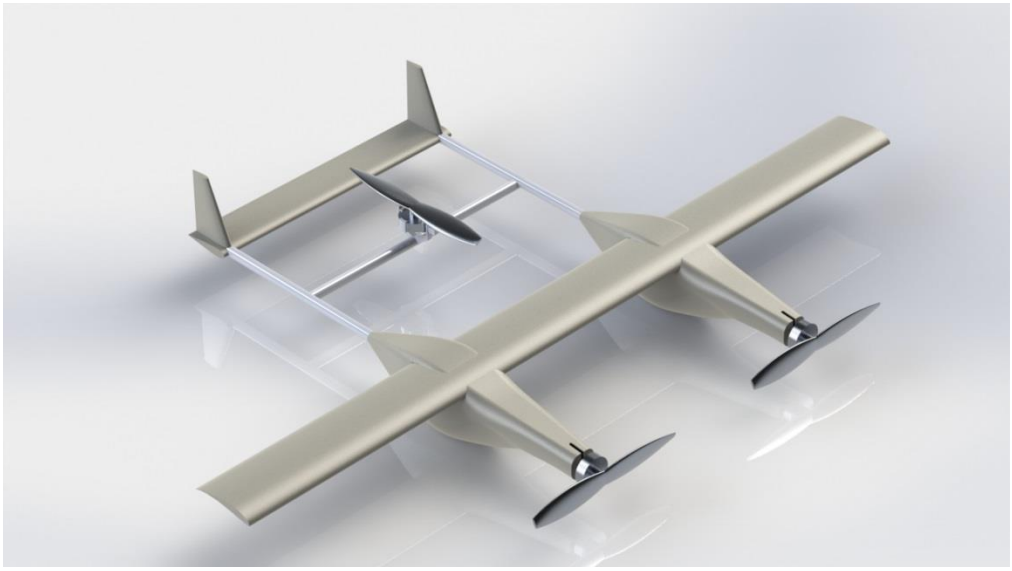

Figure C5. Rendered view of the model

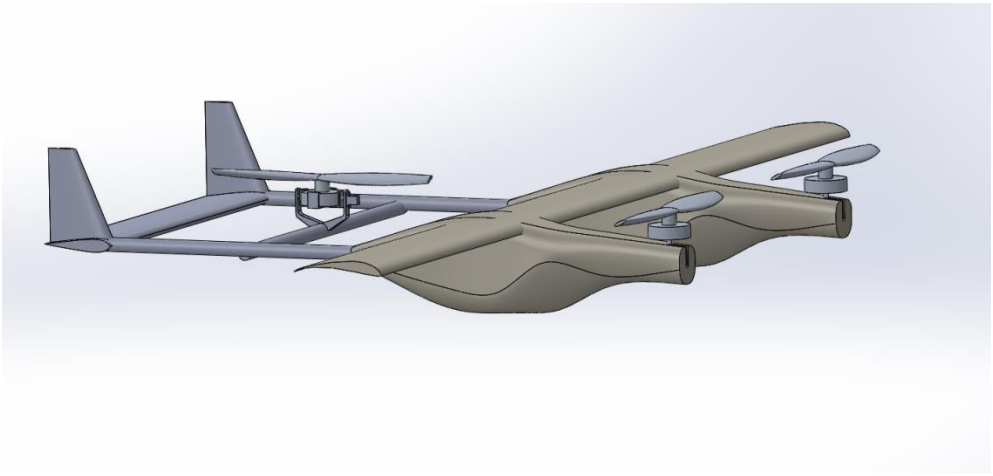

Figure C6. VTOL regime

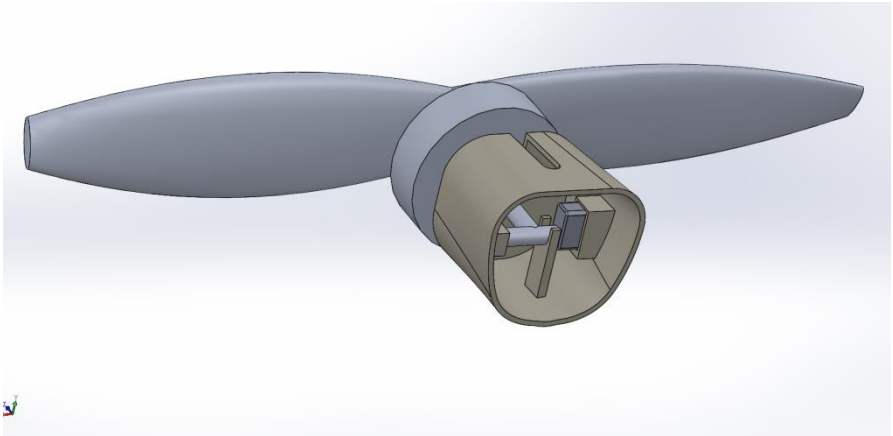

Figure C7. Front tilt rotor mechanism